Determination of VraR binding activity on promoters of *fmtA*, *murZ*, *sgtB* and *pbp2*

Zhifeng Yang

A THESIS SUBMITTED TO

THE FACULTY OF GRADUATE STUDIES

IN PARTIAL FULFILLMENT OF THE REQUIREMENTS

FOR THE DEGREE OF

MASTER OF SCIENCE

GRADUATE PROGRAM IN BIOLOGY

YORK UNIVERSITY

TORONTO, ONTARIO

August 2014

ABSTRACT

VraSR two-component system rapidly senses the cell wall damage by antibiotics and positively modulates a set of genes (VraSR Regulon) to enhance the resistance phenotype in *S. aureus*. *fmtA, murZ, sgtB* and *pbp2* are members of VraSR Regulon, and they are involved in cell wall peptidoglycan synthesis in response to cell wall inhibitors such as β-lactams. We investigated VraR binding activity on *fmtA* promoter/its mutants by *in vitro* and *in vivo* experiments. We found VraR can bind to two conserved motifs on *fmtA* promoter in the formation of a dimer and up-regulate the transcription of *fmtA* under oxacillin conditions. We also found *fmtA* had two transcription start sites: -157G was responsible for maintenance of a basal level expression, and -195G was induced by oxacillin treatment. We reported VraR/phosphorylated-VraR binding sequences on promoters of *murZ*, *sgtB* and *pbp2*. Putative transcription start sites of *murZ*, *sgtB* and *pbp2* were also identified.

ACKNOWLEDGEMENT

First, I would like to thank my supervisor, Dr. Golemi-Kotra, for her guidance, advice, commitment, encouragement, and patience in the past three years. This thesis could not have been completed without her support.

Special thanks to the chair of the oral examination committee, Dr. White, who was also the member of my thesis supervisory committee. I appreciate that he always gave valuable feedbacks to make my work better.

I appreciate the other members of my thesis examination committee: Dr. Hudak and Dr. Audette, for their constructive comments and suggestions.

I am also thankful to my colleagues in Dr. Golemi-Kotra's lab, also my forever friends: Dr. Verma, Dr. Singh, Hena, Uzma, Michael, Kevin, Mohammad and Martin. We worked together, supported each other, and got through all the difficulties and funs.

My sincere thanks go to my family. My parents' love, support and understanding motivated me to chase my dreams. I particularly thank my wife, Hong, for being my soul mate, and for always standing by me no matter ups and downs.

Additional thanks to Adrienne and Cristalina for their always reliable administrative support.

To those whom I love and those who love me, I dedicate this thesis.

TABLE OF CONTENTS

LIST OF ABBREVIATIONS

Asp	Aspartic Acid
CA-MRSA	community-acquired MRSA
EMSA	Electrophoretic Mobility Shift Assay
FPLC	Fast Protein Liquid Chromatography
HA-MRSA	hospital-acquired MRSA
His	Histidine
HK	Histidine Protein Kinase
LB	Luria-Berani Broth
MRSA	Methicillin Resistant *Staphylococcus aureus*
PBP	penicillin-binding proteins including four natural penicillin-binding proteins (PBP1, PBP2, PBP3, and PBP4) and an acquired penicillin-binding protein 2a (PBP2a)
PCR	Polymerase Chain Reaction
P*fmtA*	Promoter of *fmtA*
qRT-PCR	Real Time Quantitative Polymerase Chain Reaction
RLM-RACE	RNA Ligase Mediated Rapid Amplification of cDNA Ends
RR	Response Regulator
S. aureus	*Staphylococcus aureus*

SAB	*S. aureus* bacteremia
SDS-PAGE	SDS-polyacrylamide gel electrophoresis
TB	Terrific Broth
TCS	Two-component System
TSB	Tryptic Soy Broth
TSS	Transcription start site
VraR-P	Phophorylated VraR
VraR~P	Mixture of unphophorylated and phosphorylated VraR
VRSA	Vancomycin Resistant *Staphylococcus aureus*

CHAPTER ONE: METHICILLIN-RESISTANT *STAPHYLOCOCCUS AUREUS*

1.1 Pathogenesis and history of *Staphylococcus aureus*

S. aureus is a Gram-positive bacterium belonging to the Micrococcaceae family. The organisms appear as grape-like clusters under the microscope (Lowy 1998). *S. aureus* causes multiple serious or fatal diseases such as bacteremia, endocarditis, metastatic infections, sepsis, toxic shock syndrome, pneumonia, and even food poisoning (Lowy 1998).

Human skin, especially the anterior area of the nares, is the main reservoir of *S. aureus*. Twenty percent of the human population are so-called persistent carriers, harboring one type of *S. aureus* strain. Approximately 60% of people, known as intermittent carriers, sporadically carry different strains (Kluytmans et al. 1997).

S. aureus produces various types of virulence factors such as enzymes, toxins, or other cellular components that are involved in its ability to infect, colonize, or cause disease (Lowy 1998). *S. aureus* can secrete a wide range of enzymes depending on the strain. Hemolysins, nucleases, proteases, lipases, hyaluronidase, and collagenase may be involved in the digestion of host tissues and the spread of *S. aureus*. Some strains secrete exotoxins such as toxic-shock syndrome toxin-1, the staphylococcal enterotoxins, the

exfoliative toxins (including epidermolytic toxins A and B), and leukocidin that may impact the immune systems of hosts and have other biological functions (Dinges et al. 2000; Lowy 1998).

S. aureus was first discovered in the late 19th century and remains a common cause of infections from skin injuries or post-operative wounds in humans and other animals (Deurenberg and Stobberingh 2008). Before the use of penicillin for the treatment of *S. aureus* infections, the fatality rate reached 81.97% in 122 patients with *S. aureus* bacteremia (SAB) at Boston City Hospital (Skinner and Keefer 1941). Mortalities from SAB have declined significantly and continuously with the development of treatments, including antibiotics, in the last 70 years, but SAB is still fatal in 10-30% of patients (van Hal et al. 2012; Laupland 2013).

1.2 Methicillin-resistant *S. aureus* (MRSA)

The remarkable versatility of *S. aureus* under environmental pressure allows it to quickly acquire resistance to nearly all antibiotics used in treatments (Stryjewski 2014). The introduction of penicillin dramatically improved the prognosis of patients with *S. aureus* infections. Penicillin-resistant isolates of *S. aureus*, however, were identified in hospitals and later in communities only a few years after the medical introduction of penicillin (Rammelkamp and Maxon 1942). The resistance to penicillin was due to the production of an inducible β-lactamase (Rammelkamp and Maxon 1942; Bondi and Dietz

1945), and resistance spread quickly. By the late 1960s, more than 60% of the *S. aureus* strains in hospitals had acquired penicillin resistance, and 90% of *S. aureus* strains are now resistant through the production of β-lactamase (Finland 1955; Barber and Rozwadowska-Dowzenko 1948; Lowy 2003).

Methicillin was developed in 1959 to combat the inactivation of penicillin by β-lactamase (Lowy 2003). Methicillin was derived from penicillin and was the first semisynthetic penicillinase-resistant penicillin (Figure 1.1). Methicillin was synthesized with the phenol group of benzylpenicillin disubstituted with methoxy groups, which significantly reduced its affinity to β-lactamase (Lowy 2003).

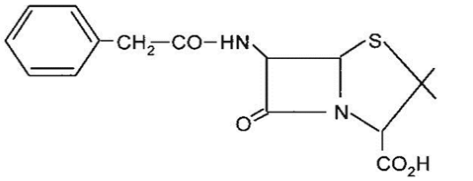

Benzylpenicillin

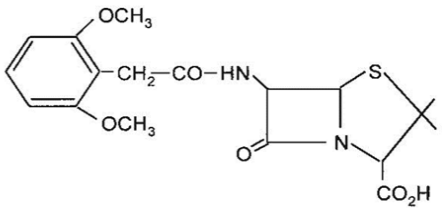

Methicillin

Figure 1.1 Chemical structure of Benzylpenicillin and Methicillin (Stapleton and Taylor 2002).

Methicillin and other β-lactams achieved great early success in treating penicillin-resistant *S. aureus*. The first MRSA strain was reported just two years after its

introduction but remained rare until the emergence of a multidrug-resistant MRSA in Europe in the 1960s (Jevons 1961; Otto 2012). Methicillin resistance is mainly due to the acquisition of the *mecA* gene from *Staphylococcus sciuri7* (Stapleton and Taylor 2002). MRSA quickly disseminated worldwide from the 1970s with the emergence of novel lineages. The percentage of MRSA resistant to methicillin, oxacillin, and nafcillin increased from 2.4% to 29% from 1975 to 1991 in US hospitals (Panlilio et al. 1992). A survey by Diekema et al. (2001) indicated that roughly 20-70% of *S. aureus* isolates were resistant to β-lactams in most countries, regardless of geographic area.

Extensive use of β-lactam antibiotics in the clinical treatment of *S. aureus* has been followed by the emergence and spread of MRSA. MRSA, originally named for the acquisition of methicillin resistance in *S. aureus* strains, have developed resistance to nearly all clinically used antibiotics, such as all β-lactams and vancomycin (Fan et al. 2007; M 2013).

The key mechanism of resistance to methicillin and other β-lactam antibiotics is based on the expression of the foreign gene *mecA*, which produces penicillin-binding protein 2a (PBP2a) (Stapleton and Taylor 2002). The targets of β-lactams are four natural penicillin-binding proteins (PBP1, PBP2, PBP3, and PBP4) that catalyze the cross-linking or transpeptidation reactions in the assembly of the peptidoglycan structure. The cell wall becomes vulnerable to internal osmotic pressure when the cross-linking of peptidoglycan

is inhibited by β-lactams, and the cells die. PBP2a has a lower penicillin-binding affinity relative to PBP2 (Pinho et al. 1998). PBP2a has similar penicillin-binding motifs as the other PBPs but much lower β-lactam binding activity, which compensates for the cross-linking of peptidoglycan under high doses of β-lactams (Stapleton and Taylor 2002).

During the 1990s, clones of community-acquired MRSA (CA-MRSA) from non-patient settings or from new patients with no history of MRSA infection were observed in Australia, Europe, North America, Latin America, and Asia. CA-MRSA, initially distinct from hospital-acquired MRSA (HA-MRSA) in phenotype, genotype, and antibiotic susceptibility, entered hospitals and merged with HA-MRSA (Deurenberg and Stobberingh 2008; Stryjewski and Corey 2014).

Since the emergence of MRSA, the glycopeptide vancomycin became the treatment of choice against MRSA. Isolates of MRSA strains with intermediate vancomycin resistances were reported in Japan and then in other countries in 1997 (Lowy 2003). The first reported vancomycin-resistant *S. aureus* strain, Mu50, was heterogeneously resistant to vancomycin and so was still sensitive to vancomycin but produced some resistant subpopulations. These strains were found in approximately 20% of the hospitals in Japan (Hiramatsu et al. 1997).

Another serious concern is complete vancomycin resistance in some MRSA strains due mainly to an acquired foreign operon, *vanA*, which modifies the cell-wall precursor D-Ala-D-Lac, the target of vancomycin, to D-Ala-D-Ala, allowing the continued synthesis of peptidoglycan in the cell wall (CDC 2002; Lowy 2003).

1.3 VraSR two-component system

The *mecA* gene, encoding the 78-kDa PBP2a in MRSA isolates, plays an essential role in resistance to β-lactams. PBP2a, however, does not fully control the resistance phenotype of MRSA, and other factors such as the VraSR two-component system (TCS) coordinate the synthesis of cell-wall peptidoglycan and play an important role in expressing resistance to cell-wall inhibitors (de Lencastre et al. 1994).

1.3.1 Two-component systems

TCSs are signal-transduction systems in bacteria and usually play important roles in the expression of virulence factors and in adaptations to environmental pressures and changes (Kawada-Matsuo et al. 2011).

The predominant mechanism of such signal-transduction systems is a pathway of phosphotransfer, and its core components are two conserved proteins, a sensor histidine protein kinase (HK) and a cognate response regulator (RR). HK, which is regulated by environmental stimuli, catalyzes autophosphorylation at a conserved histidine (His) residue, creating a high-energy phosphoryl group that is subsequently transferred to an

aspartic acid residue in the response-regulator protein. The phosphotransfer is catalyzed by the conserved regulatory domain of RR. Phosphorylation of RR induces a conformational change in the regulatory domain that activates RR, which subsequently triggers intracellular responses, most often the regulation of gene expression and enzymatic activity in some cases (Stock et al. 2000).

1.3.2 VraSR Two-component System

Exposure of *S. aureus* to inhibitors of cell-wall synthesis, e.g. β-lactams and vancomycin, is followed by dramatic changes in the transcription of a number of genes. The VraSR two-component system is capable of rapidly sensing damage to cell walls and regulating a unique set of genes known as the VraSR regulon (Gardete et al. 2006; Belcheva and Golemi-Kotra 2008).

Utaida et al. (2003) reported the existence of a cell-wall-stress stimulon that included 105 genes up-regulated by the cell-wall-active antibiotics oxacillin, bacitracin, and D-cycloserine, which inhibit different steps in peptidoglycan biosynthesis. The VraSR regulon is part of this stimulon. Similarly, Kuroda et al. (2003) identified a vancomycin-induced cell-wall-stress stimulon that included 139 genes in *S. aureus* N315, and 46 of these genes under the regulation of the VraSR two-component system were considered to belong to the VraSR regulon. Gardete et al. (2006) confirmed the existence of the VraSR regulon in MRSA and laboratory strains. The VraSR two-component system

is able to sense and regulate the expression of PBP2 in *S. aureus* and to coordinate a rapid response to enhance the resistance to peptidoglycan inhibitors (Gardete et al. 2006).

Sengupta et al. (2012) provided direct *in vivo* evidence of the VraSR regulatory mechanism previously proposed by Belcheva and Golemi-Kotra (2008). According to this mechanism (Figure 1.2), VraS is a typical HK with an N-terminal transmembrane domain and a conserved C-terminal HK core. The N-terminal transmembrane domain of VraS consists of two membrane-spanning regions that are connected by a periplasmic linker. The conserved HK core of VraS contains the dimerization domain, which has the conserved His residue, and the ATP-binding domain. VraR is a two-domain response-regulator protein containing a conserved N-terminal regulatory domain and a C-terminal DNA-binding domain, referred to as the effector domain. Environmental stimuli are transduced through the membrane to the conserved HK core domain and trigger the autophosphorylation of HK at the conserved His residue. The phosphoryl groups are rapidly transferred to the cognate RR in an RR-catalyzed reaction. Phosphorylation of VraR induces a specific conformational change and forms a dimer at the N-terminal domain. Phosphorylated VraR binds to the promoter regions of its target genes and increases the transcription levels to compensate for the damage to the structure of cell-wall peptidoglycan.

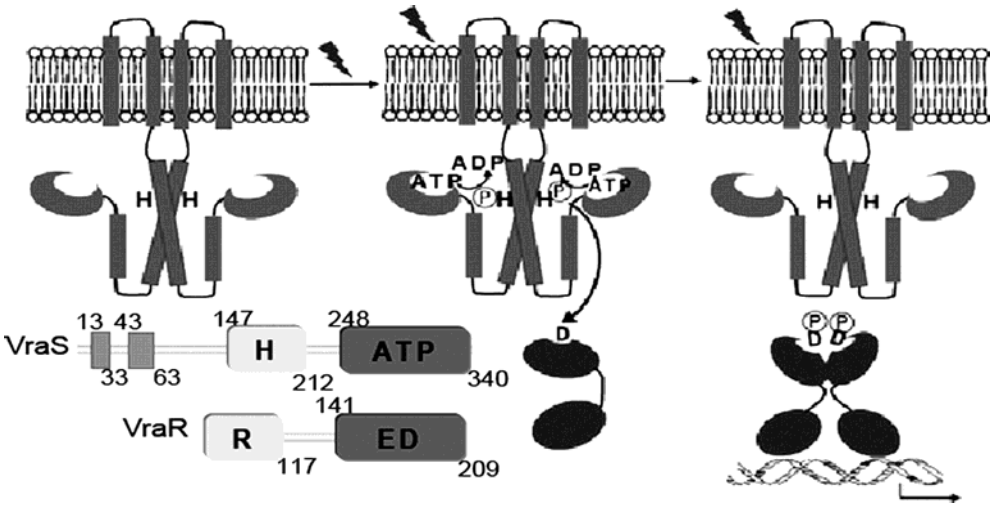

Figure 1.2 The schematic representation of VraSR two-component system(shown are the amino acid positions where the predicted domains start and end in VraS and VraR; H, the histidine box; ATP, the ATP-binding domain; R, the receiver domain; and ED, the DNA-binding domain; domain prediction by ExPaSY) (Belcheva and Golemi-Kotra 2008).

1.4 Research Objectives

Inhibitors of cell-wall synthesis, such as β-lactams and vancomycin, are still widely used in current therapies for *S. aureus* infections. A better understanding of the mechanism of MRSA resistance to these compounds may allow us to find new drug targets or to develop new antibiotics. This study focuses on the genes associated with the biosynthesis of cell-wall peptidoglycan that are under the control of the VraSR two-component system. These genes are potentially important drug targets. The VraR binding activities at the promoters of *fmtA, murZ, sgtB*, and *pbp2* and the regulatory mechanism are investigated.

CHAPTER TWO: DETERMINATION OF VRAR BINDING ACTIVITY AT THE PROMOTER OF *FMTA IN VITRO*

2.1 Introduction

2.1.1 Regulation of *fmtA* transcription under antibiotic-induced cell-wall stress

The *fmtA* gene encodes FmtA, a low-affinity penicillin-binding protein, and is a member of the VraSR regulon family involved in peptidoglycan biosynthesis under antibiotic (cell-wall inhibitors) conditions in *S. aureus* (Fan et al. 2007; Utaida et al. 2003; Kuroda et al. 2003; McAleese 2006; Muthaiyan et al. 2008). The precise function of FmtA is still unclear, but some characteristics of the *fmtA* gene and its regulatory mechanism have been clarified (Komatsuzawa 1999; McAleese et al. 2006; Zhao et al. 2012; Fan et al. 2007; Tu et al. 2007; Sengupta et al. 2012).

The level of transcription of *fmtA* increases in the presence of cell-wall inhibitors (e.g. vancomycin and β-lactams) (McAleese et al. 2006; Zhao et al. 2012; Komatsuzawa 1999). Inactivation of *fmtA* reduces the level of cross-linking in peptidoglycan and the rate of autolysis of *S. aureus* in the presence of Triton X-100 (a detergent capable of solubilizing membrane-associated proteins) (Komatsuzawa 1999). The *fmtA* mutant of *S. aureus* produces no teichoic acid and reduces biofilm formation by a structural change in the cell wall (Zhao et al. 2012; Tu et al. 2007).

2.1.2 Current understanding of VraR binding activity at the *fmtA* promoter

The *fmtA* gene is 1191 base pairs (bp) long, and its promoter region (P*fmtA*) is 450 bp immediately upstream of the translation initiation codon (ATG). All DNA fragments and sequences of *fmtA* or *PfmtA* used in this study are based on the *S. aureus* subsp. Mu50 strain, an MRSA strain with vancomycin resistance whose genome has been sequenced (Kuroda et al. 2001). The top strand in this study is the sense strand, and the bottom strand is the antisense strand. Position +1 refers to the A of the start codon ATG in the top strand, and so on.

The *fmtA* promoter has two VraR-specific binding sites, here named A1 and A2 (Figure 2.1a and 2.1b). Based on the DNase I footprinting assays, the A1 site is protected only by phosphorylated VraR, and the A2 site is protected by both phosphorylated and unphosphorylated VraR. The protection occurs on both the top and bottom strands.

Belcheva et al. (2009) found two VraR binding motifs in the *vraSR* promoter: 5'-ACT$(X)_n$AGT-3' and 5'-TGA$(X)_n$TCA-3', where X is any nucleotide and n = 1-3. A specific region, $^{-241}$ACTttAGTaTGAtgTCt^{-225}, in the A2 site is highly conserved with the VraR binding site R1 (ACTaaAGTaTGAacaTCa) in the *vraSR* promoter (Belcheva et al. 2009), and both of the two conserved regions include the two identified VraR binding motifs (Figure 2.1b). But A1 does not have similar motifs (Figure 2.1b).

Mutations at the cytosine (C) and guanine (G) nucleotides in the conserved region caused obvious decreases in the affinity of VraR binding at P*fmtA*. The Cs and Gs (underlined) in the conserved subregions 5'-A<u>C</u>TttA<u>G</u>T-3' and 5'-T<u>G</u>AtgT<u>C</u>t-3' in the full *fmtA* promoter were mutated, and the mutated subregions were then inserted into *lux* fusion plasmids, where the addition of a functional promoter region increased the expression of bioluminescent signals in *S. aureus*. Both double mutations caused a loss of up-regulation of the bioluminescent signals relative to the wild-type promoter, suggesting that VraR might bind to these two motifs in pairs (phosphorylated VraR is a dimer). I proposed that this dimer could be separated to eliminate the binding of VraR if additional nucleotides were inserted into the interior of these two motifs. I also hypothesized that the mutagenesis of C and G in the VraR binding motifs may help to reveal the VraR binding activity and motifs at A1 as it did in the *vraSR* promoter (Belcheva et al. 2009).

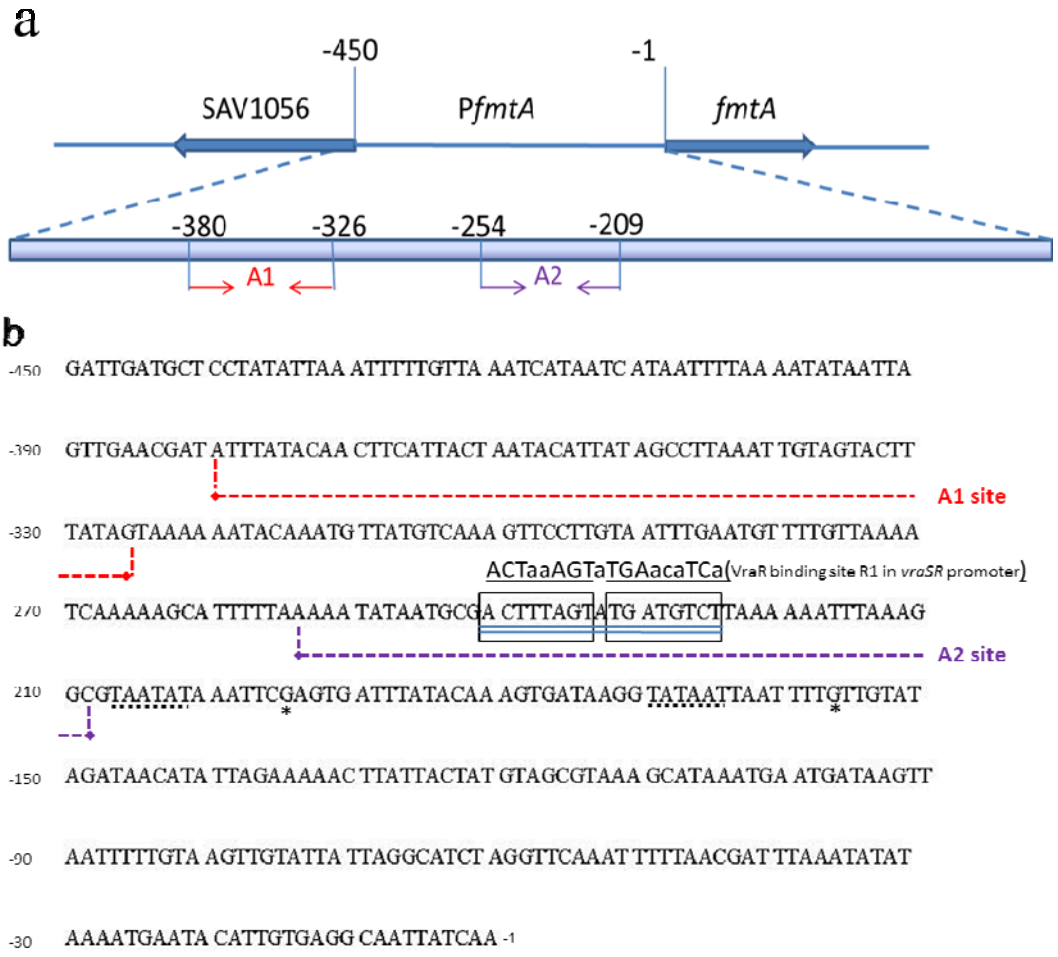

Figure 2.1 *fmtA* promoter region in the *S. aureus* strain Mu50. a) 450bp region between *fmtA* and SAV1056 genes is considered as promoter of *fmtA* (P*fmtA*). VraR binding sites A1 and A2 identified in this study are shown. b) DNA sequence of P*fmtA*. A1 and A2 sites are indicated with red and purple dash lines. Conserved VraR binding sequences (double-underlined) including two VraR binding motifs (two boxes) are shown. Two transcription start sites identified in this study are indicated with "*", and corresponding -10 regions are underlined with round dots.

2.2 Materials and Methods

2.2.1 Generation of mutants of the *fmtA* promoter

The full *fmtA* promoter (P*fmtA,* nucleotides -498 to +42) was inserted into the pSTBlue-1 blunt-ended vector (Novagen) by V. Verma in Dr. Golemi-Kotra lab. EcoRI (gccGAATTC) and BamHI (GGATCCggc) sites were added to the 5' and 3' ends of this region, respectively (unpublished). (Lower letters represent additional nucleotides added for the convenience of restriction enzyme digestion.) Six single/double mutants were generated from the above plasmid (Figure 2.2; Table 2.1). Mutant 1 (M1) possessed an additional adenine (A) at position -233 of A2 (-233A/AA). Mutant 2 (M2) had the C at -356 replaced by an A. Mutant 3 (M3) had the C at -356 and the G at -349 replaced by A and thymine (T), respectively. Mutant 4 (M4) had the Cs at -373 and -367 replaced by As. Mutant 5 (M5) had the Cs at -363 and -356 replaced by As. Mutant 6 (M6) had the G at -339 and the C at -333 replaced by T and A, respectively.

A1 (wild type)	5′ – ATTTATACAACTTCATTACTAATACATTATAGCCTTAAATTGTAGTACTTTATAG
A1-M2	5′ – ATTTATACAACTTCATTACTAATAAATTATAGCCTTAAATTGTAGTACTTTATAG
A1-M3	5′ – ATTTATACAACTTCATTACTAATAAATTATATCCTTAAATTGTAGTACTTTATAG
A1-M4	5′ – ATTTATAAAACTTAATTACTAATACATTATAGCCTTAAATTGTAGTACTTTATAG
A1-M5	5′ – ATTTATACAACTTCATTAATAATAAATTATAGCCTTAAATTGTAGTACTTTATAG
A1-M6	5′ – ATTTATACAACTTCATTACTAATACATTATAGCCTTAAATTTTAGTAATTTATAG
A2 (wild type)	5′ – AAAATATAATGCGACTTTAGTATGATGTCTTAAAAAATTTAAAGGC
A2-M1	5′ – AAAATATAATGCGACTTTAGTAATGATGTCTTAAAAAATTTAAAGGC

Figure 2.2 Sequences of VraR binding-sites A1 and A2 in P*fmtA* and there mutants. Five mutants were derived from the A1 site: M2, M3, M4, M5 and M6. One mutant was derived from the A2 site: M1. Underlined sequences indicate the targeted mutation sites and the red-highted sequences indicate mutated nucleotides in each mutant.

Table 2.1 Primers designed for the generation of six mutants of the *fmtA* promoter by Quikchange™ Site-direct Mutagenesis Kit (Stratagene). Red-highlighted letters indicate the mutated nucleotides.

Primer name	Primer sequence	Mutations
A2A22AA FWD	5’ – GCGACTTTAGTAATGATGTCTTAAAAAATTTAAAGGC	M1, -233A/AA
A2A22AA REV	5’ – GCCTTTAAATTTTTTAAGACATCATTACTAAAGTCGC	
A1C22A FWD	5’ – CTTCATTACTAATAAATTATAGCCTTAAATTGTAGTACTTTATAG	M2, -356C/A
A1C22A REV	5’ – CTATAAAGTACTACAATTTAAGGCTATAATTTATTAGTAATGAAG	
A1C22A/G29T FWD	5’ – CTTCATTACTAATAAATTATATCCTTAAATTGTAGTACTTTATAG	M3, -356C/A& -349G/T
A1C22A/G29T REV	5’ – CTATAAAGTACTACAATTTAAGGATATA	

	ATTTATTAGTAATGAAG	
A1C5A/C11A FWD	5' – GTTGAACGATATTTATAAAACTTAATTA CTAATACATTATAGCC	M4, -373C/A& -367C/A
A1C5A/C11A REV	5' – GGCTATAATGTATTAGTAATTAAGTTTTA TAAATATCGTTCAAC	
A1C16A/C22A FWD	5' – GATATTTATACAACTTCATTAATAATAAA TTATAGCCTTAAATTG	M5, -363C/A& -356C/A
A1C16A/C22A REV	5' – CAATTTAAGGCTATAATTTATTATTAATG AAGTTGTATAAATATC	
A1G39T/C45A FWD	5' – GCCTTAAATTTTAGTAATTTATAGTAAA AAATACAAATGTTATG	M6, -339G/T& -333C/A
A1G39T/C45A REV	5' – CATAACATTTGTATTTTTTACTATAAATT ACTAAAATTTAAGGC	

The QuikChange™ Site-Directed Mutagenesis Kit (Stratagene) was used for the mutagenesis. Primers designed for generation of mutagenisis were shown in Table 2.1. The following PCR conditions were used: 95 °C for 2 min, 16 cycles of 95 °C for 45 s, 55 °C for 1 min, 68 °C for 6.5 min, and a final extension step of 68 °C for 5 min. PCR-amplified plasmids were digested by DpnI and then transformed by heat shock into NovaBlue competent *E. coli* cells that were grown on LB plates containing 50 μg/mL kanamycin. Colonies were picked, and the plasmids were extracted using Qiagen plasmid mini kit and then examined by DNA sequencing.

2.2.2 Purification and Phosphorylation of VraR

The *vraR* gene had previously been inserted into the pET26b vector, which had then been transformed into *E. coli* BL21 (DE3) expression cells (Belcheva et al. 2009). The cells were grown in TB (define acronym) medium, and protein expression was induced by 0.4 mM IPTG (define acronym) at 25 °C for 16 h. The cell pellet was dissolved in equilibration buffer (20 mM Tris and 5 mM $MgCl_2$, pH 7.0). After sonication, the supernatant was loaded onto a DEAE Sepharose column and then eluted by elution buffer (500 mM Tris and 5 mM $MgCl_2$, pH 7.0). Fractions containing VraR were loaded onto heparin-Sepharose columns and then eluted by the same elution buffer as above. The collected fractions containing VraR were concentrated by Ultra 10K filters (Amicon; 10,000 NMWL). The final concentration of VraR was determined by a Bradford assay after electrophoresis on a 15% SDS-PAGE gel.

VraR was phosphorylated as described previously (Belcheva et al. 2009), with slight modifications. $MgCl_2$ and lithium potassium acetyl phosphate dissolved in phosphorylation buffer (50 mM Tris-base, pH 7.4, 50 mM KCl, and 5 mM $MgCl_2$) were mixed with 150 µM VraR to obtain a solution containing 100 µM VraR, 20 mM $MgCl_2$, and 50 mM lithium potassium acetyl phosphate. The reaction was incubated at 37 °C for 1 h, and phosphorylation activity was confirmed by electrophoresis on a 10% native polyacrylamide gel. The content of phosphorylated VraR (VraR-P) under our

experimental conditions was approximately 70% (Belcheva and Golemi-Kotra 2008). VraR~P thus refers to a mixture of phosphorylated and unphosphorylated VraR.

2.2.3 DNase I footprinting assays to investigate the VraR binding activity at the *fmtA* promoter and its mutants

The target DNA fragment, -394 to -199 of the *fmtA* promoter region, referred to as seq1-3 which contains both A1 and A2 sites, was PCR-amplified using the forward primer 5'-ATTAGTTGAACGATATTTATAC and the reverse primer 5'-GAATTTATATTACGCCTTTAAAT. The following PCR conditions were used: 95 °C for 2 min, 30 cycles of 95 °C for 20 s, 55 °C for 30 s, 72 °C for 30 s, and a final extension step of 72 °C for 5 min. A target fragment A1S (from -425T to -299T, containing only A1) was PCR-amplified using the forward primer 5'- TGTTAAATCATAATCATAAT and the reverse primer 5'- ACTTTGACATAACATTTG. The same PCR conditions were used as the PCR-amplification of seq1-3.

All amplified DNA fragments were purified using the QIAquick Gel Extraction Kit (Qiagen) and used as PCR templates in DNase I footprinting assays. The 5'end of the primer of interest (the forward primer for the investigation of the top strand or the reverse primer for the investigation of the bottom strand) was labeled with [γ-^{32}P] ATP (3000 Ci/mmol) using 20 U of T4 polynucleotide kinase (NEB) and was used to amplify seq1-3 in a 20-µL reaction. Binding reactions were prepared in binding buffer (10 mM Tris, pH

7.5, 50 mM KCl, and 1 mM DTT) supplemented with 5 mM $MgCl_2$, 0.05% herring sperm DNA, and 2.5% glycerol. The end-labeled DNA (6-15 ng) was mixed with VraR/VraR~P at concentrations ranging from 0 to 40 μM. Binding reactions were incubated for 30 min at room temperature and then digested with DNase I (0.024 U/reaction) for 2 min. The digestions were stopped by adding 50 μL of DNase I stop solution (1% SDS, 0.2 M NaCl, and 20 mM EDTA, pH 8.0). Digested DNA samples were extracted by phenol-chloroform and then precipitated with ethanol. Purified DNA was resuspended in loading dye containing 10 mM formamide, 1 mg/mL bromophenol blue, and 1 mg/mL xylene cyanol, heated at 95 °C, and electrophoresed on an 8% polyacrylamide gel containing 7 M urea. The dried gels were exposed to phosphor screens and scanned using a Typhoon Trio+ variable-mode imager (GE HealthCare). The C and G sequencing reactions for these experiments were performed in 10-μL PCR reactions containing 1 μL of end-labeled primer, 0.5 μL of Therminator DNA polymerase, 50 nM dNTPs, 1.9 μM acyGTP or acyCTP, and 25 ng of template DNA (gel-purified seq1-3).

2.2.4 Electrophoretic mobility shift assay (EMSA)

The target DNA fragments were generated with synthesized primers (Sigma) (Table 2.2). A1a, A1b and A1c, derived from the A1 site, were defined in Table 2.2.

Table 2.2 Primers (5’ to 3’) used to generate double-stranded DNA fragments for the EMSAs. The red-highlighted letters represent the mutated nucleotides.

Primer	Primer sequences	Position of annealed dsDNA fragment in P*fmtA*

fmtAPtopA1	GATATTTATACAACTTCATTACTAATACATTATAGCCTTAAATTGTAGTACTTTATAGTAA	Region -383 to -323, containing the full VraR binding-site A1 in P*fmtA*
fmtAPbotA1	TTACTATAAAGTACTACAATTTAAGGCTATAATGTATTAGTAATGAAGTTGTATAAATATC	
fmtAPtopA2	TTAAAAATATAATGCGACTTTAGTATGATGTCTTAAAAAATTTAAAGGC	Region -257 to -209, containing the full VraR binding-site A2 in P*fmtA*
fmtAPbotA2	GCCTTTAAATTTTTTAAGACATCATACTAAAGTCGCATTATATTTTTAA	
fmtAPtopM1	TTAAAAATATAATGCGACTTTAGTAATGATGTCTTAAAAAATTTAAAGGC	Full VraR binding-site A2 in P*fmtA*, containing M1, -233A/AA
fmtAPbotM1	GCCTTTAAATTTTTTAAGACATCATTACTAAAGTCGCATTATATTTTTAA	
fmtAPtopM4	GATATTTATAAAACTTAATTACTAATACATTATAGCCTTAAATTGTAGTACTTTATAGTAA	Full VraR binding-site A1 in P*fmtA*, containing M4, -373C/A & -367C/A
fmtAPbotM4	TTACTATAAAGTACTACAATTTAAGGCTATAATGTATTAGTAATTAAGTTTTATAAATATC	
fmtAPtopM6	GATATTTATACAACTTCATTACTAATACATTATAGCCTTAAATTTTAGTAATTTATAGTAA	Full VraR binding-site A1 in P*fmtA*, containing M6, -340G/T & -333C/A
fmtAPbotM6	TTACTATAAATTACTAAAATTTAAGGCTATAATGTATTAGTAATGAAGTTGTATAAATATC	
fmtAP A1aTop	GATATTTATACAACTTCATTACTAATAC	A1a, part of the VraR binding-site A1 in P*fmtA*, -383 to -356
fmtAP A1aBot	GTATTAGTAATGAAGTTGTATAAATATC	
fmtAP A1aTopM4	GATATTTATAAAACTTAATTACTAATAC	Ala containing M4

fmtAP A1aBotM4	GTATTAGTAATTAAGTTTTAT AAATATC	
fmtAP A1bTop	ATTATAGCCTTAAATTGTAG TACTTTATAGTAA	A1b, part of the VraR binding-site A1 in P*fmtA*, -355 to -323
fmtAP A1bBot	TTACTATAAAGTACTACAAT TTAAGGCTATAAT	
fmtAP A1bTopM6	ATTATAGCCTTAAATTTTAGT AATTTATAGTAA	A1b containing M6
fmtAP A1bBotM6	TTACTATAAATTACTAAAAT TTAAGGCTATAAT	
fmtAP A1cTop	TGAACGATTAATACATTATA AAAAATA	A1c, containing part of the VraR binding-site A1 in P*fmtA*, including regions -388 to -381, -361 to -352, & -325 to -317
fmtAP A1cBot	TATTTTTTATAATGTATTAAT CGTTCA	

VraR/VraR~P binding affinities with seq1-3 were also investigated by EMSAs. The seq1-3 was obtained by PCR using the primers: 5'-ATTAGTTGAACGATATTTATAC-3' and 5'-GAATTTATATTACGCCTTTAAAT-3'. The following PCR conditions were used: 95 °C for 2 min, 30 cycles of 95 °C for 20 s, 55 °C for 30 s, 72 °C for 30 s, and a final extension step of 72 °C for 5 min. The amplified DNA fragments were purified by QIAquick Gel Extraction Kit (Qiagen).

The DNA fragments (1.245 pmol) were labeled with [γ-^{32}P]ATP (3000 Ci/mmol) using T4 polynucleotide kinase. Binding reactions (20 µL) were prepared in binding buffer (10 mM Tris, pH 7.5, 50 mM KCl, and 1 mM DTT) supplemented with 5 mM $MgCl_2$, 10 ng of herring sperm DNA, and 2.5% glycerol. Target DNA (0.03 pmol) was mixed with protein concentrations varying from 0 to 35 µM. The reaction mixtures were incubated at 25 °C for 30 min and electrophoresed on 8%-10% native polyacrylamide

gels (seq1-3 on 8% gels and primer-annealed DNA fragments on 10% gels). Dried gels were exposed to phosphor screens (GE HealthCare), with the time of exposure depending on the remaining level of radioactivity. The gel was then scanned by a Typhoon Trio+ variable-mode imager (GE HealthCare) and analyzed by ImageJ software. K_d was defined as the concentration of VraR/VraR~P (μM) required to shift 50% of the input DNA.

2.3 Results

Gs and Cs normally play an important role in typical VraR binding motifs, and mutations of G or C nucleotides significantly decrease the affinity of VraR binding to the corresponding motifs (Belcheva et al. 2009). By closely examining the features of the VraR binding-site A1 of the *fmtA* promoter, I predicted which Gs or Cs were essential for the binding of VraR. Variants containing mutations of these Gs and Cs were generated, and the effects of these mutations on VraR binding activity were investigated by *in vitro* and *in vivo* experiments (Figure 2.2). A highly conserved VraR binding region was identified on the VraR binding-site A2. An A had been inserted into this motif, and I hypothesized that this additional nucleotide would interrupt the formation of phosphorylated VraR dimers.

2.3.1 Generation of fusion plasmids containing P*fmtA* mutants

A fusion plasmid had previously been prepared by inserting the *fmtA* promoter region -498 to +42 into the pSTBlue-1 vector by Belcheva in Dr. Golemi-Kotra lab. Five

single- or double-nucleotide mutants (M2-M6) targeted to VraR binding-site A1 were derived from this plasmid to investigate the role of the Gs and Cs. One single-nucleotide mutant (M1) targeted to VraR binding-site A2 was also derived. All mutations were confirmed by sequencing (Figure 2.2).

2.3.2 Purification of VraR

Wild-type VraR was purified in a two-step protocol. Peak fractions containing VraR were collected at elution-buffer contents of 20-30% on a DEAE sepharose column and were then loaded onto a heparin-Sepharose column (Figure 2.3a). In the second step, purified VraR was observed in the peak fractions at elution-buffer contents of 40-60% (Figure 2.3b). Purified VraR was stored at 4 °C, which maintained stability for 2-4 weeks.

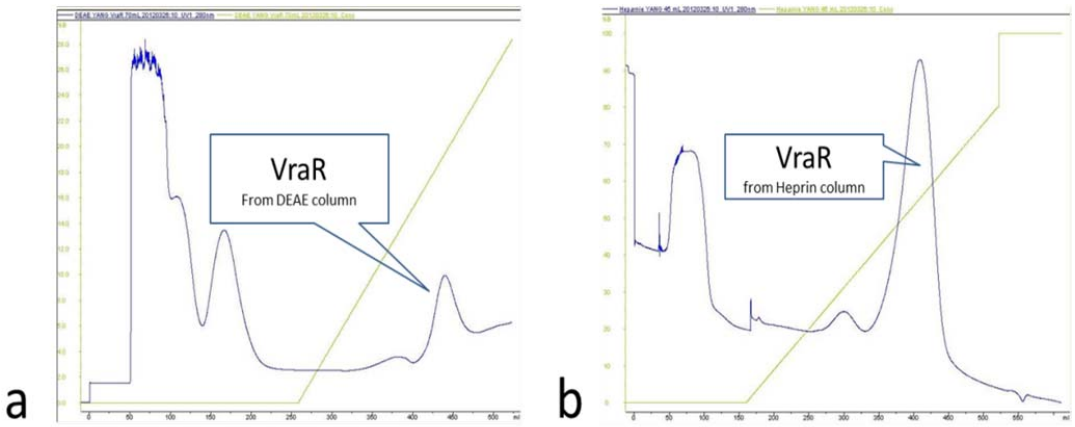

Figure2.3 Typical procedure of purification of VraR by FPLC. (a) first-step purification by DEAE sepharose column. The peak containing VraR is typically observed around 20% to 30% of elution buffer. (b) second-step purification by Heparin sepharose column. The peak (λ280nm) contains pure VraR was typically observed around 40% to 60% of elution buffer. Y axis: Content of elution buffer (%); X axis: Order numbers of collection tubes; The blue and yellow lines represent protein absorbance at λ 280nm and content of elution buffer (%).

2.3.3 DNase I footprinting assays

The VraR binding-site A1 had previously been determined to be protected only by VraR~P, and A2 was protected by both VraR and VraR~P (A. Belcheva in Dr. Golemi-Kotra lab, unpublished).

VraR binding-site A1 in P*fmtA* was protected only by VraR~P in the DNase I footprinting assays, and the site had little sequence similarity with the previously identified VraR binding motifs in the *vraSR* promoter (Belcheva et al. 2009). Since G and C usually play an important role in VraR binding (Belcheva et al. 2009), I generated five mutants to investigate whether VraR~P binding activity was affected by mutation of the putatively essential nucleotides (Figure 2.2). Replacement of -373C and -367C (M4) reduced VraR~P binding activity at A1 from -380 to -363 of the top strand and from -378 to -366 of the bottom strand (Figure 2.4 and 2.6). Replacement of -339G and -333C (M6) had a similar effect on VraR~P binding activity at A1 from -339G to -326G of the top strand and from -345T to -329A of the bottom strand (Figure 2.5 and 2.6). Both M4 and M6 decreased VraR~P binding activity at sequences near -356C. The effect of M4 and M6 at A1 was much weaker than the effect of M1 on VraR binding at A2 (Figure 2.7). The other mutants (M2, M3, and M5) had no significant effect on VraR/VraR~P binding compared to the wild type (data not shown).

I found a VraR binding region in A2 that was similar to the VraR binding site R1 in the *vraSR* promoter: $^{-241}$ACTttAGTaTGAtgTCt^{-225}. VraR bound as a dimer at this site (Figure 2.1b). The double mutations -240C/-235G or -231G/-226C prevented increases in *fmtA* expression under oxacillin treatment (add initial of first name Verma in Dr. Golemi-Kotra lab, unpublished). I investigated the effect of M1 on VraR binding activity and on the ability of VraR to bind as a dimer. The insertion of an A after -233 separated these two VraR binding motifs. An investigation of the bottom strand of seq1-3 indicated that VraR and VraR~P protected the same region from -251 to -225 from DNase I digestion. Interestingly, M1 caused an almost complete loss of both VraR and VraR~P binding activity at the A2 site, but the A1 site was not affected by M1 (Figure 2.7).

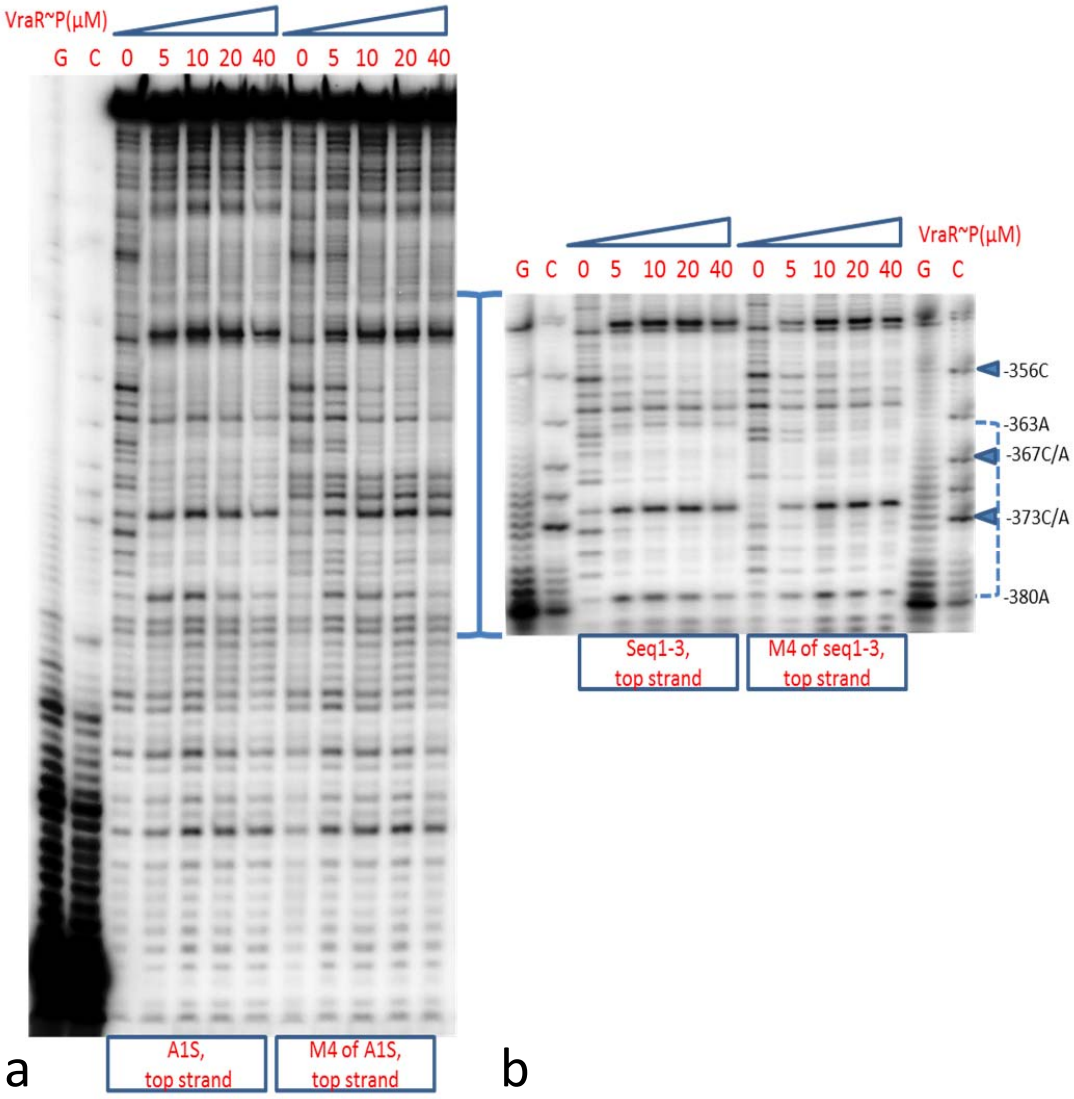

Figure 2.4 DNase I footprinting assays showed VraR~P binding activity on the top strands of DNA fragments containing A1 site or its mutant M4.
(a)VraR~P binding activity on the top strand of A1S (from -425T to -299T, contains A1 site only) and its mutant M4. (b) VraR~P binding activity on the top strand of seq1-3 (-394 to -199, containing both A1 and A2) and its mutant M4. (only M4-affected region was shown). Blue solid lines indicate same region containing M4-affected region on both target DNA fragments. The dashed line indicates M4-affected region (from –380A to –356C). –356C is a single nucleotide affected by M4. –373C/A and –367C/A indicate two mutated nucleotides of M4. Lane G and C represent the G/C ladders, respectively.

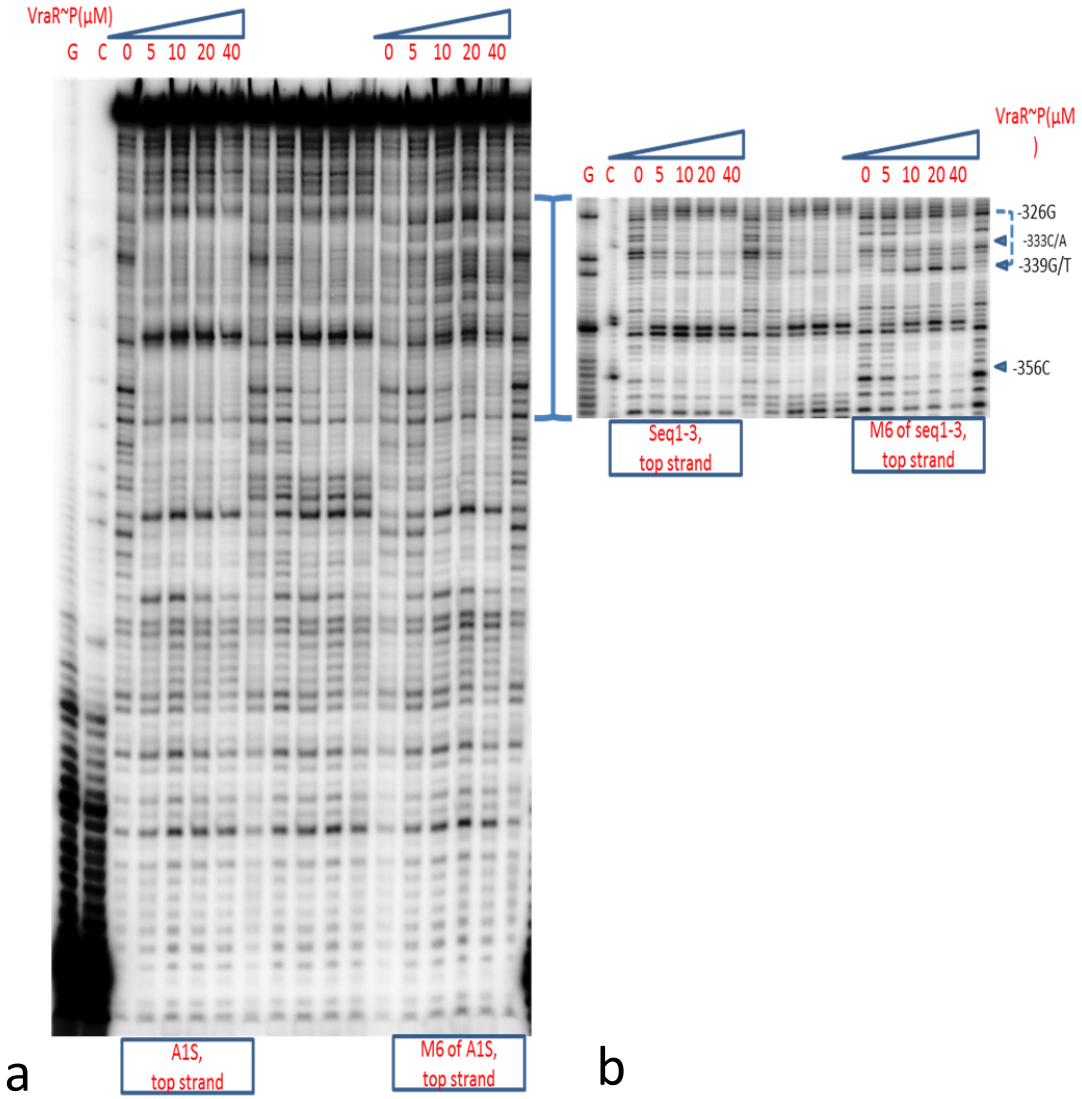

Figure 2.5 DNase I footprinting assays showed VraR~P binding activity on the top strands of DNA fragments containing A1 site or its mutant M6.
(a)VraR~P binding activity on the top strand of A1S (from -425T to -299T, contains A1 site only) and its mutant M6. (b) VraR~P binding activity on the top strand of seq1-3 (-394 to -199, containing both A1 and A2) and its mutant M6. (only M6-affected region was shown). Blue solid lines indicate same region containing M6-affected region on both target DNA fragments. The dashed line indicates M6-affected region (from –339G to –326G). –356C is a single nucleotide affected by M6. –333C/A and –339G/T indicate two mutated nucleotides of M6. Lane G and C represent the G/C ladders, respectively.

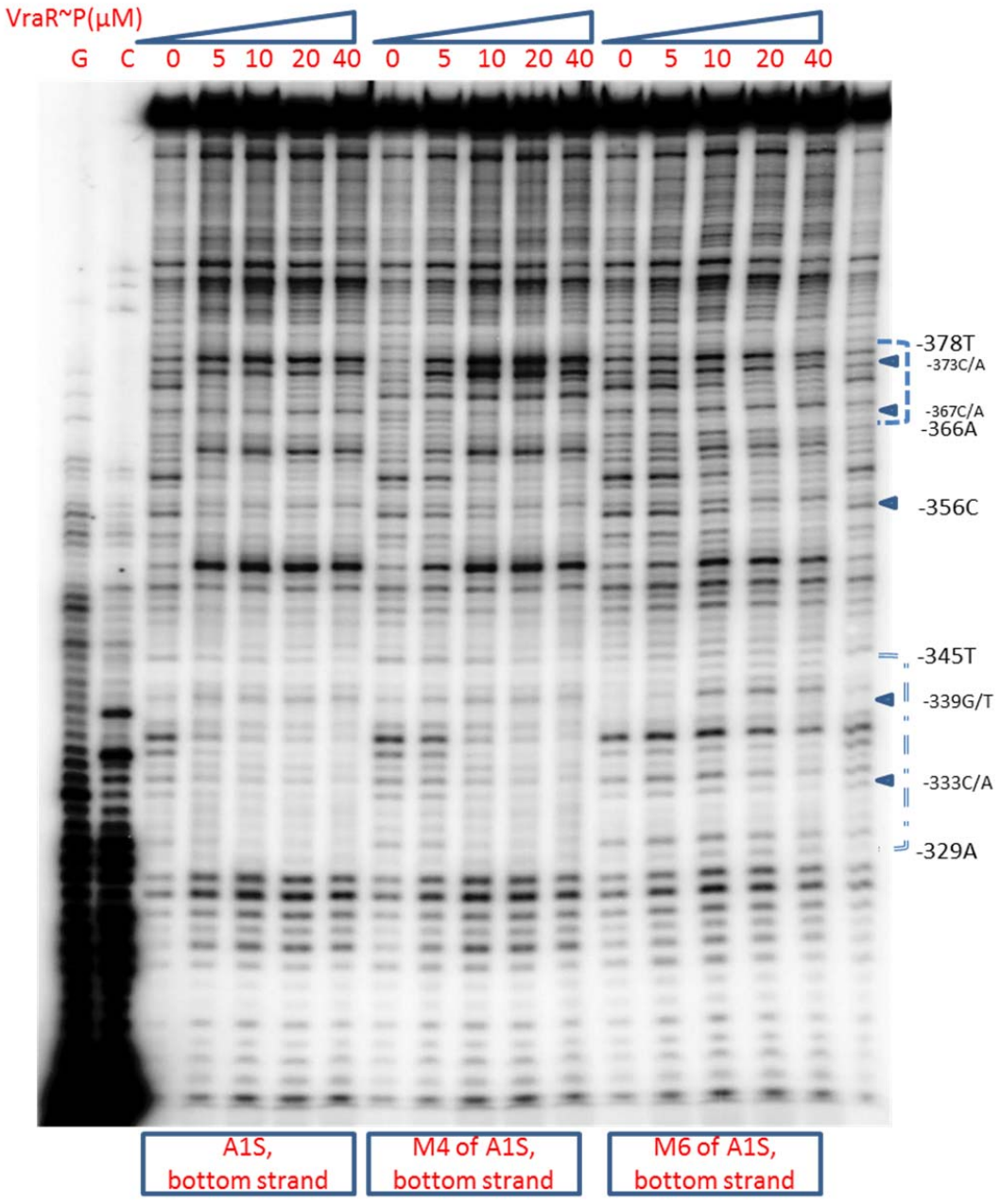

Figure 2.6 DNase I footprinting assays showed VraR~P binding activity on bottom strands of A1S (from -425T to -299T) containing A1 site or its mutant M4/M6. The dash-dot line indicates the M6-affected region (from –345T to –329A), and the dashed line indicates the M4-affected region (from –378T to –366A). –356C represents a single nucleotide affected by both M4 and M6. –373C/A and –367C/A indicate two mutated nucleotides of M4. –339G/T and –333C/A indicate two mutated nucleotides of M6. Lane G and C represent the G and C ladders, respectively.

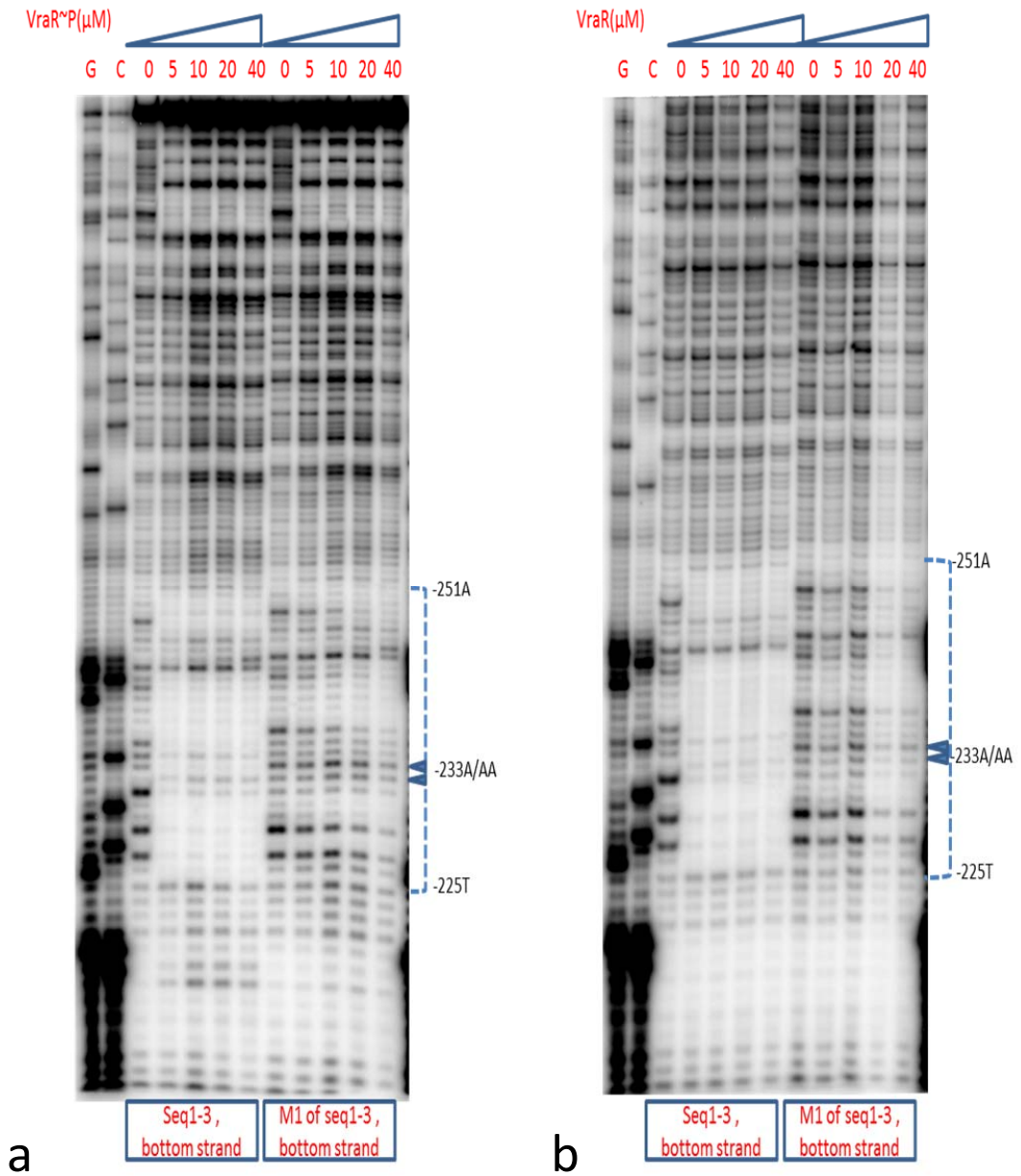

Figure 2.7 DNase I footprinting assays showed VraR~P and VraR binding activity on bottom strands of seq1-3 containing A2 site or its mutant M1.
(a) VraR~P binding activity on the bottom strands of seq1-3 and its mutant M1. (b) VraR binding activity on the bottom strands of seq1-3 and its mutant M1. Dashed lines indicate M1-affected regions (the same region, from –251A to –225T, affected by M1 on both gels). Double-arrowheads indicate the mutated nucleotide on M1 where one Adenine is replaced by two Adenines. Lane G and C represent G and C ladders, respectively.

2.3.4 Electrophoretic mobility shift assay (EMSA)

EMSA assays investigated the effect of three P*fmtA* mutants, M1, M4, and M6, on the binding affinity of VraR/VraR~P at P*fmtA* (Figure 2.8 and Appendix Figure3). These mutants decreased VraR/VraR~P binding in the DNase I footprinting assays.

The insertion of an Adenine in A2 (mutant A2-M1) significantly decreased the binding affinities of VraR (K_d value increased from 5.9±0.12 to 12.3±2.52 μM) and VraR~P (K_d value increased from 5.6±0.12 to 9±0.89 μM) at the A2 site (Figure 2.8). A1-M4 and A1-M6 caused no obvious change in VraR~P binding affinity relative to the affinity at the wild-type A1 site.

The K_d values of VraR/VraR~P binding at the seq1-3 were 7.2±0.5 μM and 5.5±1.02 μM, respectively, which were close to the K_d values of VraR/VraR~P binding at the A2 site, while significantly lower than that of the A1 site (Figure 2.8). According to the data of DNase I footprinting assays, A1a region is affected by M4, A1b is affected by M6, and A1c is affected by both M4 and M6 when DNase I digestion occurs. Three short DNA fragments were derived from A1 based on the regions affected by M4/M6 in the DNase I footprinting assays (Figure 2.9). A1a contained the region affected by M4, A1b contained the region affected by M6, and A1c contained the interior region of A1 that was affected by both M4 and M6. To look closely at the VraR binding activity in the A1 site, EMSA assays were also conducted to investigate VraR/VraR~P binding affinities at A1a,

A1b, and A1c (Figure 2.9). A1a containing M4 and A1b containing M6 were also generated by primer annealing and were used in the EMSA assays (Table 2.2). All DNA fragments had very low VraR~P binding affinity, and K_d values could not be determined, because they were beyond the range of the protein concentrations on the EMSA gels (Figure 2.10 and Appendix Figure 1). No VraR binding activity was observed for any of the fragments. Binding activity did not differ between the wild-type fragments and their mutants.

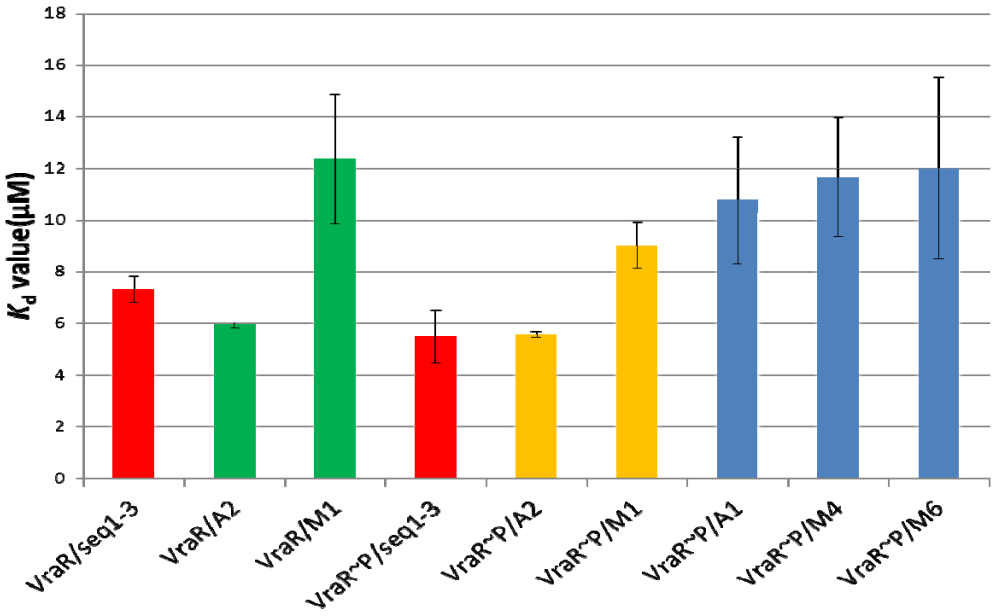

Figure 2.8 EMSA analysis of the DNA-binding affinities of VraR/VraR~P to seq1-3, A1, A2 and their variants (representative gels shown in Appendix Figure 3). Red columns indicate VraR/VraR~P binding to seq1-3. Green columns indicate VraR binding to A2 and its mutant M1. Yellow columns indicate VraR~P binding to A2 and its mutant M1. Blue columns indicate VraR~P binding to A1 and its mutants M4 and M6. Means of K_d values and standard deviations were calculated from at least three independent experiments. K_d was defined as the concentration of VraR/VraR~P (μM) required to shift 50% of the input DNA.

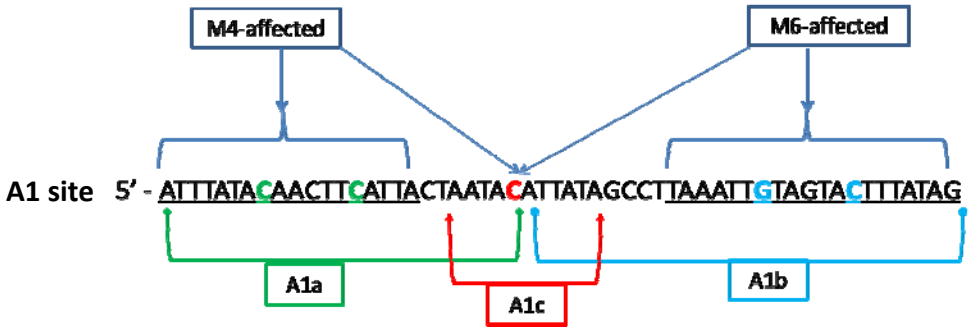

Figure 2.9 M4-affected and M6-affected regions within the VraR binding site A1 are shown. A1a, A1b and A1c contain nucleotides on upstream and/or downstream of A1 site to obtain longer DNA fragments for EMSA assays. Green-highlighted nucleotides indicate where the mutation occurs on M4. Blue-highlighted nucleotides indicate where the mutation occurs on M6. All the fragments used in EMSA were obtained by primer annealing method.

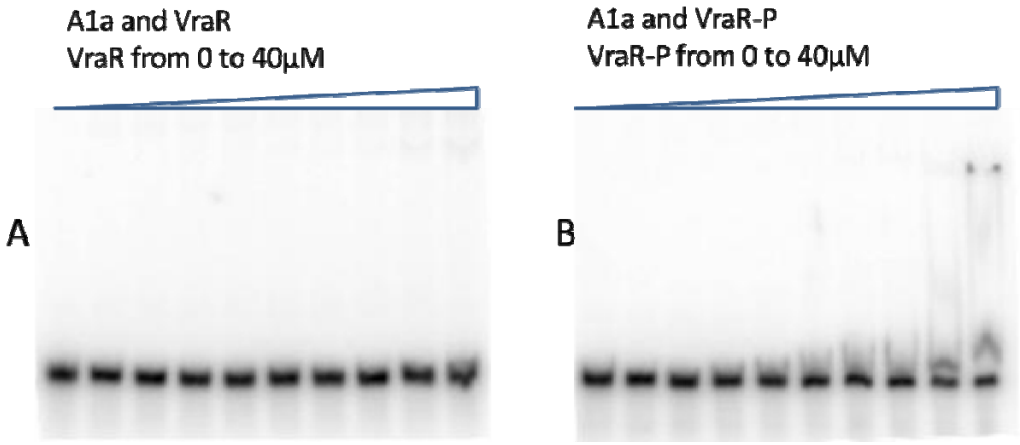

Figure 2.10 Investigation of VraR/VraR~P binding affinity on A1a by EMSA. A1a-M4, A1b, A1b-M6 and A1c showed similar gel patterns. Rest images shown in Appendix Figure 1. K_d values could not be determined accurately due to the range of available protein concentrations prepared in EMSA procedure.

2.4 Discussion

The A2 site in P*fmtA* had two VraR binding motifs, which were highly conserved with previously identified binding motifs in the VraR binding site R1 of the *vraSR* promoter (Belcheva et al. 2008). The entire A2 site lost the protection by VraR or VraR~P under DNase I digestion when an A was inserted between these two motifs, suggesting that the inserted nucleotide may have separated the dimerized VraR or changed its structural conformation so that it lost the ability to bind to A2. I propose that two VraR monomers are able to bind to two binding motifs independently, in agreement with the protection of A2 from DNase I digestion by unphosphorylated VraR. The loss of protection from DNase I digestion by both VraR and VraR~P caused by the inserted nucleotide between the two motifs, however, suggests that only the VraR dimer can bind to A2, and when the dimerization is disrupted by the inserted nucleotide, the ability of the VraR monomers to bind to specific motifs is lost or dramatically decreased. When unphosphorylated, the two VraR monomers may not be able to bind to A2 unless they are able to form a dimer.

A1 had fewer conserved features in its sequence and was only protected by phosphorylated VraR. The effects of mutants M2-M6 on VraR binding to A1 were much weaker than the effect of M1 on VraR~P binding to A2, suggesting that A2 may be the major functional site responsible for the regulation of *fmtA* transcription by VraR. I

observed no interference between A1 and A2 on the DNase I footprinting gels, and these two sites appear to have no interaction when VraR binds to the promoter.

The EMSA assays indicated that M1 significantly decreased the binding affinity of VraR/VraR~P at A2, while mutations in A1 had no effect. VraR~P had very low binding affinities to the short fragments (A1a, A1b, and A1c) derived from A1, and VraR did not bind even at VraR concentrations as high as 40μM. Mutations in A1a and A1b had no effect, perhaps suggesting that phosphorylated VraR had the ability to bind to A1, but the binding was weak and may not have been very specific, which was consistent with the findings from the DNase I footprinting assays that mutations in A1 had little or no effect on the VraR~P protection pattern.

CHAPTER THREE: DETERMINATION OF VRAR BINDING ACTIVITY AT *FMTA* PROMOTER *IN VIVO*

3.1 Introduction

Previous *in vitro* results indicated that M1 significantly influenced VraR binding activity at A2, while mutations in A1 had little effect. To further elucidate the binding activity of VraR, I performed *in vivo* experiments to confirm the effect of the mutants M1, M4, and M6, which had some effect on VraR binding to P*fmtA*, on the interaction between VraR and P*fmtA*. Because the mutations in A1 did not affect the expression of *fmtA* relative to the wild type, I wanted to determine if the deletion of the entire A1 site from P*fmtA* would affect expression under oxacillin treatment.

Francis et al. (2000) constructed a novel vector (*lux* plasmid/pXEN1) by adding a modified *luxABCDE* cassette (genes required for the expression of bioluminescent signals) to the pMK4 plasmid. This vector normally does not express bioluminescent signals due to the lack of a promoter region, but the restriction sites in the plasmid allow the addition of foreign promoters. The effectiveness of inserted foreign promoters could be easily determined by measuring the intensity of the bioluminescent signals. I constructed *lux* fusion plasmids by inserting P*fmtA* and mutants into the *lux* plasmid to test the differences in *in vivo* expression caused by the mutations.

An *fmtA* complementary strain had previously been produced in our lab. The *fmtA* gene was deleted from the genome of the RN4220 strain of *S. aureus*, and the loss of FmtA *in vivo* was complemented by a fusion plasmid constructed by inserting the *fmtA* gene and its 450-bp promoter region into a pMK4 expression vector. Modifications to P*fmtA* to explore its features were easily made, and the data from *in vivo* experiments reflected the true behavior of VraR more directly.

3.2 Materials and Methods

3.2.1 Bioluminescence expression assay and the construction of *luxABCDE* fusion strains with derivatives of the P*fmtA* region

The regions of P*fmtA* and its mutants from -498 to +42 were amplified from pSTBlue-1 vectors containing the *fmtA* promoter (-498 to +42) or its mutants by primers containing EcoRI and BamHI restriction sites at their 5' ends (DirFmtAP 5'-gccgaattcGAGAACCAATGCTAGAAGGATC and RevFmtAPr 5'-gccggatccTACACACGCATGTATAACTAGT, respectively) and ligated into the pXEN1 vector by T4 DNA ligase (NEB). Both the P*fmtA* fragment and the pXEN1 vector were double-digested with EcoRI and BamHI (NEB) and purified using the QIAquick Gel Extraction Kit (Qiagen) before ligation. The plasmids were transformed into NovaBlue cells by heat shock (42 °C, 1 min) and into RN4220 by electroporation (2 kV, 2.5 ms) using a Micropulser (Bio-Rad). Positive colonies were confirmed by plasmid

sequencing. The M1, M4, and M6 mutants of the *fmtA* promoter were produced, as described in Chapter 2.

For the bioluminescence expression assay, 200 µL of an overnight culture of each target strain were added to 20 mL of TSB medium and incubated at 37 °C and 200 rpm to an OD_{600nm} of approximately 0.4. Two 5-mL aliquots of the culture were then prepared, one received 10 µg/mL oxacillin and the other served as a control and both were incubated at 37 °C and 200 rpm for 30 min. At least three replicates of 300-µL aliquots from each sample were added to an opaque 96-well plate, and the bioluminescent signal was measured by a Synergy H4 plate reader with integral measurement for 100 ms at a luminescence height of 1 mm.

3.2.2 Deletion of target fragments in pXEN1 containing the *fmtA* promoter

All methods for deleting DNA fragments in plasmids in this study were modified from Pérez-Pinera et al. (2006) (Figure 3.1). To delete the entire A1 site (-380 to -326), the deletion-primers DirPfmtAA1de2 and RevPfmtAA1de2 containing NdeI restriction sites at their 5' ends (Table 3.1) were used to amplify the plasmid but delete the target fragment. The PCR used 10 pg of plasmid template (pSTBlue-1 containing the *fmtA* promoter at -498 to +42), 2.5 U *PfuTurbo* DNA polymerase, 1X *PfuTurbo* buffer, 0.3 mM dNTPs, and 0.4 µM of each primer in a 50-µL reaction. The amplification product was gel-extracted and digested with DpnI and NdeI. The digested product was gel-purified

again and then ligated into pSTBlue-1 by T4 DNA ligase at 22 °C for 20 min. The plasmids, referred to as P*fmtA*$^{A1-}$::pSTBlue-1, were then transformed by heat shock (42 °C, 2 min) into NovaBlue competent cells that were grown on LB plates containing 50 µg/mL ampicillin. Deletion was confirmed by plasmid sequencing.

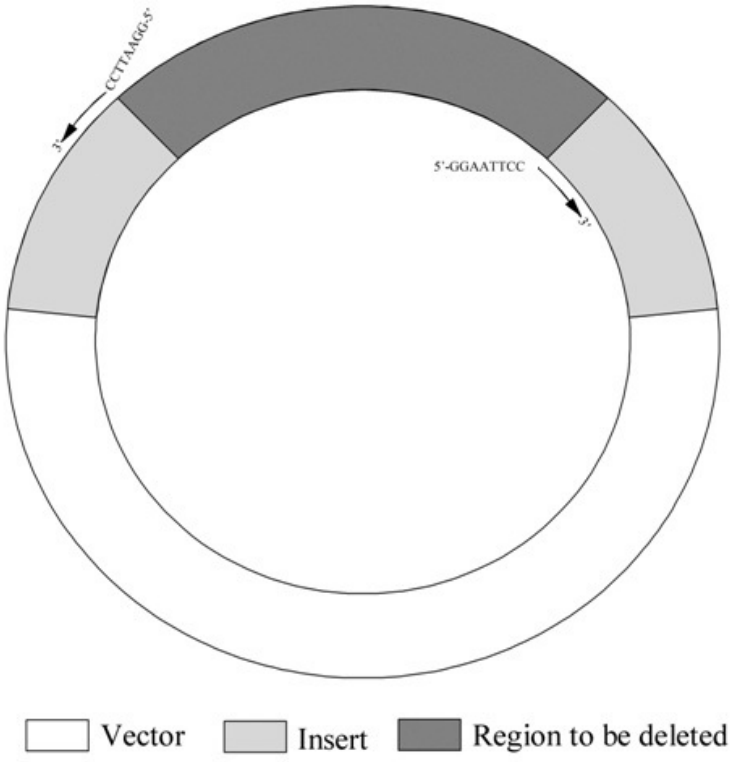

Figure 3.1 Schematic diagram to illustrate the how the primers were designed containing the sequence of the restriction enzyme at the 5' end and with the 3' end oriented so that the polymerase will amplify the entire plasmid,but notthe region to be deleted (Pérez-Pinera et al. 2006). 5'-GGAATTCC represents the selection of restriction enzyme sites at the 5'end of designed primers and this is absentin the plasmid.
As the result, the target region is replaced by selected restriction enzyme sites or removed from the plasmid if no restriction enzyme sites are selected.

The region of P*fmtA* (-498 to +42) containing the A1 deletion (-380 to -326 deleted) was amplified from the above plasmid by primers containing EcoRI and BamHI restriction sites at their 5' ends (DirFmtAP 5'-gccgaattcGAGAACCAATGCTAGAAGGATC and RevFmtAPr 5'-gccggatccTACACACGCATGTATAACTAGT, respectively) and ligated into the pXEN1 vector by T4 DNA ligase (NEB). Both the P*fmtA* fragment and the pXEN1 vector were double-digested with EcoRI and BamHI (NEB) and purified using the QIAquick Gel Extraction Kit (Qiagen) before ligation. The plasmids were transformed into NovaBlue cells by heat shock (42 °C, 1 min) and into RN4220 by electroporation (2 kV, 2.5 ms) using a Micropulser (Bio-Rad). Positive colonies were confirmed by plasmid sequencing.

3.2.3 Deletion/mutation of target fragments of the *fmtA* promoter in pMK4 containing fmtA and its promoter region

3.2.3.1 Single-site mutagenesis of pMK4 containing *fmtA* and its promoter

Mutant M1 (-233A/AA) of the VraR A2 binding site was generated in pMK4 containing *fmtA* and its promoter using the QuikChange™ Site-Directed Mutagenesis Kit (Stratagene). Two primers, 5' -GCGACTTTAGTAATGATGTCTTAAAAAATTTAAAGGC and

5’ – GCCTTTAAATTTTTTAAGACATCATTACTAAAGTCGC, were used to PCR-amplify pMK4 plasmids containing *fmtA* and its promoter region (-450 to -1). The products were digested with DpnI and then transformed by heat shock into NovaBlue competent cells that were grown on LB plates containing 50 µg/mL ampicillin. Mutation was confirmed by plasmid sequencing. The plasmids containing the expected mutation were transformed into the RN4220 Δ*fmtA* strain by electroporation. Colonies were picked from TSB plates supplied with 20 µg/mL chloramphenicol, and the mutations were confirmed by plasmid sequencing.

3.2.3.2 Deletion of target fragments in pMK4 containing *fmtA* and its promoter

To delete the entire A1 site (-380 to -326), the deletion primers DirPfmtAA1del and RevPfmtAA1del with SmaI restriction sites at their 5’ ends (Table 3.1) were used to amplify the plasmid but delete the target fragment. The PCR used 2 pg of plasmid template (pMK4 containing *fmtA* and its promoter), 2.5 U *PfuTurbo* DNA polymerase, 1X *PfuTurbo* buffer, 0.3 mM dNTPs, and 0.4 µM of each primer in a 50-µL reaction. The amplification product was gel-extracted and digested with DpnI and SmaI. The digested product was gel-purified again and then ligated with T4 DNA ligase at 22 °C for 20 min. (An alternative method is to digest the PCR product with DpnI only and mix equal volumes of End conversion buffer provided with the pSTBlue-1 vector and the gel-extracted DNA at 22 °C for 15 min and then add T4 DNA ligase at 22 °C for 20 min.)

The plasmids were transformed by heat shock (42 °C, 2 min) into NovaBlue competent cells that were grown on LB plates containing 50 µg/mL ampicillin. Deletion was confirmed by plasmid sequencing. The plasmids containing the expected deletion were then transformed into the RN4220 Δ*fmtA* strain by electroporation. Colonies were picked from TSB plates supplied with 20 µg/mL chloramphenicol, and the deletions were confirmed by plasmid sequencing.

Table 3.1 Primers used to generate mutations (deletion/replacement of targeted sequences in P*fmtA*) in plasmids. Letters highlighted in red represent restriction sites added to the 5' end of each primer to replace the targeted sequences with the restriction sites.

Primer	Primer sequence	Mutant generated
DirPfmtAA1del	5'-TCCCCCGGGTAAAAAATACAAATG TTATG	Deletion of A1 site in pMK4
RevPfmtAA1del	5'-TCCCCCGGGATCGTTCAACTAATTA TAT	
DirPfmtAA1de2	5'-GGGAATTCCATATGTAAAAAATACA AATGTTATG	Deletion of A1 site in pXEN1
RevPfmtAA1de2	5'-GGGAATTCCATATGATCGTTCAACT AATTATAT	

3.2.4 Isolation of total RNA from *S. aureus* strains

One hundred and sixty microliters of overnight cultures of each target strain were added to 16 mL of TSB medium and incubated at 37 °C and 200 rpm in a 50-mL Falcon

tube to an OD_{600nm} of approximately 0.4. Two 5-mL aliquots of the cultures were then prepared, one received 10 μg/mL oxacillin and the other served as a control and both were incubated for 30 min at 37 °C and 200 rpm. Total RNA was isolated from the *S. aureus* strains using the RNeasy Mini Kit (Qiagen), with minor modifications of the supplied protocol. One milliliter of the *S. aureus* cultures were vigorously mixed with 2 mL of RNAprotect Bacteria Reagent (Qiagen) for 10 s and centrifuged at 5000 X g for 10 min at 4 °C after resting for 5 min. The pellets were resuspended in 200 μL of buffer containing 180 μL of TE buffer (30 mM Tris and 1 mM EDTA, pH 8.0) and 20 μL of lysostaphin (1.25 mg/mL) and incubated at room temperature for 30 min. One microliter of proteinase K (NEB) was added, and the suspensions were incubated at room temperature for 30 min, then 700 μL of buffer RLT were added, and the suspensions were vortexed for 15 s. The samples were transferred to 2-mL tubes containing glass beads and vortexed vigorously three times for 20 s with 20-s rests. The samples were centrifuged at 18000 X g for 1 min, and 700 μL of the supernatants were transferred to new 2-mL tubes and mixed with 470 μL of 100% ethanol. The samples were loaded onto RNeasy Mini spin columns and centrifuged at 8000 X g for 20 s and then washed once with 350 μL of buffer RW1 and twice with 500 μL of buffer RPE. The samples were recentrifuged for 1 min to remove all possible solution residues in the column. Total RNA was eluted with 50

µL of distilled water, and 5000 ng of the RNA were digested with 4 U DNase I in a 50-µL reaction for 20 min at 37 °C. The DNase I was inactivated at 75 °C for 10 min.

3.2.5 qRT-PCR to investigate the level of *fmtA* transcription in *S. aureus* RN4220 and its derived strains

cDNA was synthesized using the High Capacity RNA-to-cDNA kit (Life Technologies) from 500 ng of total RNA digested with DNase I. For qRT-PCR, a 20-µL reaction was prepared containing 10 µL of SYBR SELECT Master Mix (Life Technologies), 0.25 µM each primer, and 25 ng of cDNA template. PCR reactions were performed on a Rotor-gene Q qRT-PCR cycler (Qiagen) under the following conditions: 50 °C for 2 min; 95 °C for 10 min; 40 cycles of 95 °C for 15 s, 60 °C for 30 s, and 72 °C for 30 s; and a final extension step at 72 °C for 10 min (Zhao et al. 2012). Two primers were designed to specifically amplify the targeted fragment on *fmtA*: FmtADir 5' TGGTACGAAAAAGTATCCAGATG and FmtARev 5' CCAAAGAATCCCCCGTTAAG. Specific primers were also designed targeting the 16s RNA gene: 16S-RNADir 5' GCTAAGTGTTAGGGGGTTTCC and 16S-RNARev 5' TTCAACCTTGCGGTCGTACT.

3.3 Results

3.3.1 Bioluminescence assays

pXEN1 plasmids with wild-type or mutant (M1, M4, and M6) P*fmtA* were referred to as *lux* fusion plasmids: P_{fmtA}::*lux*, P_{fmtA}^{M1}::*lux*, P_{fmtA}^{M4}::*lux*, and P_{fmtA}^{M6}::*lux*, respectively. The RN4220 strains of *S. aureus* with the above plasmids were referred to as *lux* fusion strains: RN(P_{fmtA}::*lux*), RN(P_{fmtA}^{M1}::*lux*), RN(P_{fmtA}^{M4}::*lux*), and RN(P_{fmtA}^{M6}::*lux*), respectively. RN4220 with the stock pXEN1 vector was referred to as RN(::*lux*). RN4220 with pXEN1 with the A1-deleted P*fmtA* (the VraR binding-site A1 deleted from P*fmtA*) was referred to as RN(P_{fmtA}^{A1-}::*lux*). In the P_{fmtA}^{A1-}::*lux* plasmid, the A1 site was replaced by CATAATG.

All *lux* fusion plasmids with wild-type or mutant P*fmtA* but without oxacillin treatment produced bioluminescent signals of similar strengths in RN4220 (Figure 3.2). The signal strengths for the above strains treated with oxacillin, except for RN(P_{fmtA}^{M1}::*lux*), were approximately 2-fold higher. The stronger signals suggested that M1 effectively caused the loss of up-regulation at the *fmtA* promoter by VraR upon oxacillin treatment, while M4 and M6 had no effect, consistent with the previous *in vitro* results. The average signals from RN4220 with M4 and M6 were slightly higher than those from RN4220 with wild-type P*fmtA* after oxacillin treatment, but this trend was not consistent for each trial (Figure 3.2). Different concentrations of oxacillin (10 ng/μL or

100 ng/μL) had little effect on the trend of signal change with or without oxacillin treatment (Figure 3.2).

Mutant M1 of VraR binding-site A2 in P*fmtA* caused the loss of protection upon DNase I digestion *in vitro* and the loss of up-regulation of *fmtA* by oxacillin treatment *in vivo*. Mutations in A1 had a weak effect on VraR binding to P*fmtA in vitro*, but these mutations had no significant effect on the expression level of *fmtA in vivo* (Figure 3.2). I hypothesized that A1 may not be essential for VraR binding, or it may be a non-specific binding site. To determine the importance of A1 on the expression of *fmtA* regulated by VraR, I deleted A1 from P*fmtA* and determined its effect with the bioluminescence and qRT-PCR assays.

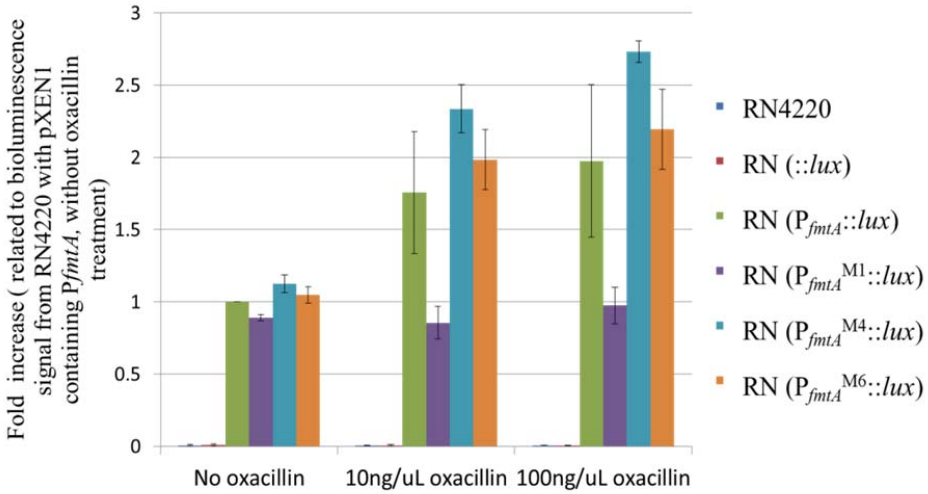

Figure 3.2 Fold increase of bioluminescence signals obtained from *lux* fusion strains under different treatments (no oxacillin, 10ng/μL oxacillin, and 100ng/μL oxacillin). The bioluminescence signal obtained from RN(P_{fmtA}::*lux*) under no oxacillin conditons was indexed to one. Bars indicate mean ± SD. The standard deviations were calculated from three independent experiments.

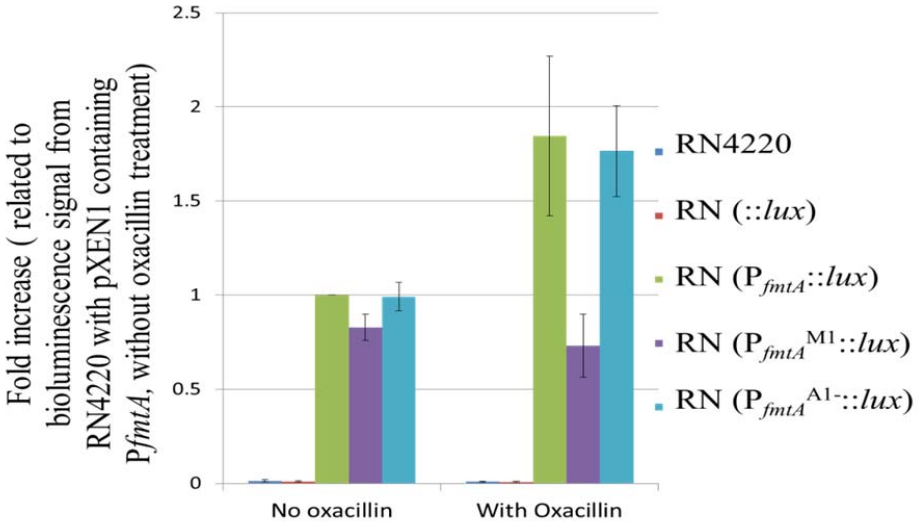

Figure 3.3 Fold increase of bioluminescence signals obtained from *lux* fusion strains. The bioluminescence signal obtained from RN(P_{fmtA}::*lux*) under no oxacillin conditions was indexed to one. Bars indicate mean ± SD. The standard deviations were calculated from three independent experiments. Deletion of entire A1 site didn't affect the bioluminescence signal expression in comparison to the wild type.

The strengths of the bioluminescent signals without oxacillin treatment were similar for the A1 deletion and RN4220 with the wild-type P*fmtA*, but the signals increased 1.77- and 1.85-fold, respectively, after oxacillin treatment (Figure 3.3). The patterns of expression in these two strains did not significantly differ. RN(P_{fmtA}^{M1}::*lux*) served as a control in these trials and provided results similar to those earlier in this study.

3.3.2 qRT-PCR for the deletion of A1 in P*fmtA*

Two mutated strains of RN4220 had previously been produced in our lab: RN4220 Δ*vraR* strain (RN4220 Δ(*vraR*)) and RN4220 Δ*vraS* (RN4220 Δ(*vraS*)). The *vraR* and

vraS genes were mutated in the genomes of these two strains, preventing the expression of the VraR and VraS proteins *in vivo*. qRT-PCR assays were conducted to investigate the effects of these mutations in *vraR* or *vraS* on *fmtA* expression *in vivo* (Figure 3.4a). The mutations had no effect on the levels of transcription of *fmtA* without oxacillin treatment. The level of transcription of *fmtA* was up-regulated 5.24-fold in the oxacillin-treated RN4220 wild-type but was not up-regulated in either of the oxacillin-treated mutated strains (Figure 3.4a).

To investigate the role of A1 and A2 in *fmtA* expression, I performed qRT-PCR to determine the *fmtA* transcription levels with and without oxacillin treatment. The pMK4 plasmids with *fmtA* and its wild-type promoter, M1, and the A1 deletion were referred to as pMK4 fusion plasmids: *fmtA*::pMK4, $fmtA^{M1}$::pMK4, and $fmtA^{A1-}$::pMK4, respectively. The RN4220 *fmtA*-mutated strains with the above plasmids were referred to as *fmtA* complementary strains: RN^{fmtA-}(*fmtA*::pMK4), RN^{fmtA-}($fmtA^{M1}$::pMK4), and RN^{fmtA-}($fmtA^{A1-}$::pMK4), respectively. In the $fmtA^{A1-}$::pMK4 plasmid, the A1 site was replaced by CCCGGG.

The transcription of *fmtA* in the RN^{fmtA-}($fmtA^{A1-}$::pMK4) strain increased 4.75-fold after oxacillin treatment, similar to the wild-type strain (Figure 3.4b). The expression of *fmtA* did not change significantly in the *fmtA* complementary strain containing M1 in P*fmtA* either with or without oxacillin treatment (Figure 3.4c).

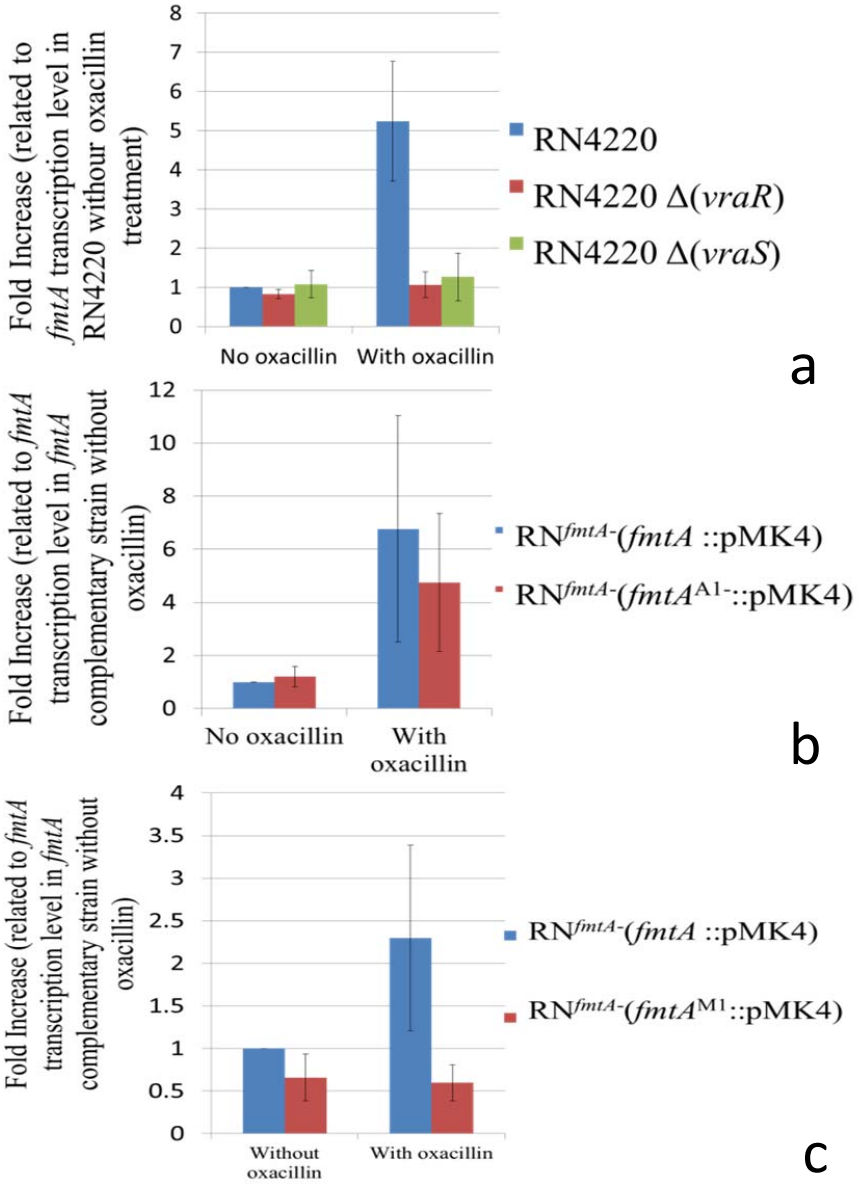

Figure 3.4 qRT-PCR results to investigate the *fmtA* transcription levels in different *S. aureus* strains. (a) Comparison of RN4220 and its *vraR* and *vraS* mutants. (b) Comparison of RN4220 complementary strain and its A1-deletion mutant. (c) Comparison of RN4220 complementary strain and its mutant M1. The *fmtA* transcription was normalized to housekeeping gene 16S-RNA gene. The *fmtA* transcription in RN4220 without oxacillin treatment was indexed to one in figure 3.4a and the *fmtA* transcription in RN^{fmtA-}(*fmtA*::pMK4) without oxacillin treatment was indexed to one in figure 3.4b and c. Bars indicate mean ± SD. The standard deviations were calculated from three independent experiments.

3.4 Discussion

The *in vivo* studies (bioluminescence and qRT-PCT assays) showed similar trends with the *in vitro* studies. The *lux* fusion strains with M4 and M6 responded similarly to oxacillin treatment as did the strain with wild-type P*fmtA*, and the increases in the levels of the bioluminescent signal and *fmtA* transcription in the qRT-PCR were near or higher than 2-fold, while strains with M1 did not respond to oxacillin treatment.

As expected, the deletion of A1 did not significantly change the level of *fmtA* expression in the A1-deleted strain relative to the wild-type strain in both experiments, suggesting that A1 was not essential to *fmtA* up-regulation under oxacillin treatment. A1 may thus not be involved in *fmtA* regulation or is not a major regulation site. VraR binding-site A2 was the major binding site in P*fmtA*. With oxacillin treatment, phosphorylated VraR could bind to the two conserved motifs in A2 of P*fmtA* and up-regulate *fmtA* expression to compromise the effect of oxacillin.

The study of the RN4220 Δ*vraR* and Δ*vraS* mutants confirmed that *fmtA* belonged to the VraSR regulon family. Both VraR and VraS were essential for the up-regulation of *fmtA* expression in response to oxacillin-induced environmental stress.

CHAPTER FOUR: DETERMINATION OF THE TRANSCRIPTION START SITE OF *FMTA*

4.1 Introduction

The transcription start site (TSS) of *fmtA* had previously been determined to be -156T by *in vitro* runoff transcription assays (Zhao et al. 2012). The RNA polymerase (RNAP) used in the assays, however, was from *E. coli*, not *S. aureus*. The differences between the RNAPs from *E. coli* and *S. aureus* prompted us to confirm if -156T was the true or only TSS of *fmtA* in *S. aureus*.

4.2 Materials and Methods

4.2.1 Determination of the TSS of *fmtA* by FirstChoice™ RLM-RACE Kit

Total RNA was isolated from *S. aureus* RN4220 using the RNeasy Mini Kit (Qiagen) as described in Chapter 3. FirstChoice™ RLM-RACE Kit (Ambion) was used to determine the TSS of *fmtA*. The protocol in this study was slightly modified from the standard procedure provided with the kit.

RNA Ligase Mediated Rapid Amplification of cDNA Ends (RLM-RACE) is a PCR-based technique used to determin the TSS in this study (Figure 4.1). The supplied adapter containing sequences corresponding to two nested sense primers is ligated to the 5' end of mRNA. A random-primed reverse transcription procedure and followed PCR

amplification by using these two antisense primers specific to the target gene provide DNA fragments with high specificity and the TSSs will be determined by subsequent DNA sequencing.

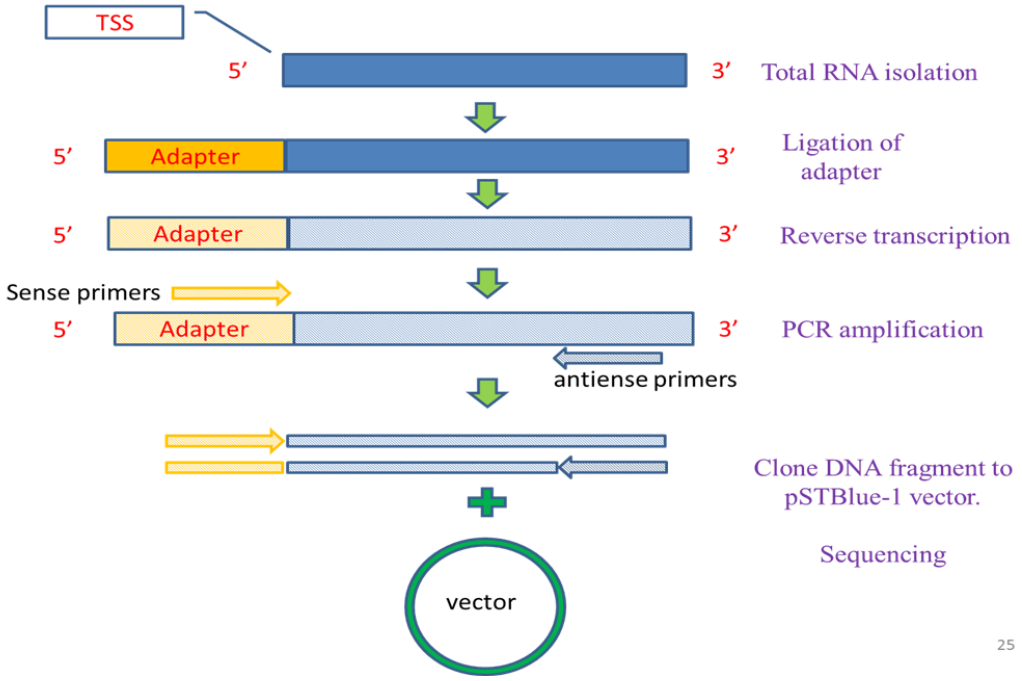

Figure 4.1 A schematic procedure of RLM-RACE in this study to determine the transcription start site of *fmtA*. TSS: Transcription start site. Adapter: a 45 base RNA adapter oligonucleotide, provided with the kit to ligate to the mRNA, nested two sense primer sequences facilitating following PCR amplification. Vector: pSTBlue-1 in this study. Dark-blue horizontal bars: RNA fragments. Light-blue horizontal bars: DNA fragments.

Total RNA treated with DNase I was precipitated with 2.5 volumes of isopropanol and 70% ethanol and then resuspended in 11 µL of distilled water. Ten-microliter reactions were prepared with 10 µg of RNA, 1 µL of TAP buffer, and 1 µL of TAP and

then incubated at 37 °C for 1 h. A 10-µL reaction was prepared with 5 µL of TAP-treated RNA, 1 µL of 5’ RACE adapter, 1 µL of RNA ligase buffer, and 2 µL of T4 RNA ligase (2.5 U/µL) and incubated at 37 °C for 1 h. A 20-µL reverse-transcription reaction was prepared with 2 µL of ligated RNA, 4 µL of dNTPs, 2 µL of random decamers, 1 µL of RNase inhibitor, 1 µL of RT buffer, and 1 µL of M-MLV Reverse Transcriptase and incubated at 42 °C for 1 h. A manually designed primer, PfmtAouterRev 5’-AACCTTTTCCTTATTACGAT, and the 5' RACE Outer Primer provided with the kit were used for the PCR amplification. A manually designed primer, PfmtAinnerRev 5’-TGTGTCTTCGTCTGTAATCG, and the 5' RACE Inner Primer provided with the kit were used for the secondary amplification of the first PCR product. The PCR product was inserted into the pSTBlue-1 vector that was then transformed into NovaBlue cells, as described in the manual, and colonies were picked and analyzed by plasmid sequencing.

4.2.2 Determination of the TSS of *fmtA* by primer extension

Total RNA was isolated from the target *S. aureus* strains, and 30-100 µg were dissolved in 60 µL of hybridization buffer (40 mM PIPES, pH 6.4, 1 mM EDTA, 0.4 M NaCL, and 80% (v/v) formamide) at 65 °C. For each strain, 0.5 pmol of primer RevFmtAEx1 5’- AATGATAAATAATAGTACACACGC or of primer RevFmtAEx2 5’- AACCTAGATGCCTAATAATACAAC labeled with [γ-^{32}P]ATP (3000 Ci/mmol) was added, and the solution was incubated at 95 °C for 5 min for denaturation and then at

45 °C for 4 h for annealing. The samples were precipitated with ethanol and dissolved in 9 µL of distilled water, and the following components were added: 0.75 µL of RNasin, 0.75 µL of dNTPs (20 mM), and 0.75 µL of D-actinomycin (4 mg/mL). After incubation at 42 °C for 2 min, 1.3 µL (13 U) of AMV-RT were added, and the mixture was incubated at 42 °C for 2 h. The reaction was terminated by adding 25 µL of stop buffer (100 µg/mL RNase A and 30 µg/mL herring sperm DNA in TE buffer, pH 8.0) and incubating at 37 °C for 30 min. After ethanol precipitation, the samples were dissolved in 7 µL of loading buffer (10 mM NaOH, 1 mM EDTA, 0.05% xylene cyanol and bromophenol blue, and 80% formamide) and electrophoresed on an 8% polyacrylamide sequencing gel. The gel was dried under vacuum and exposed to a phosphor screen for 18-24 h. A phiX 174 DNA/HinfI dephosphorylated marker (Promega) labeled with [γ-^{32}P]ATP (3000 Ci/mmol) was used to indicate the position of the RNA transcription product of *fmtA*. The RevFmtAEx2 primer labeled with [γ-^{32}P]ATP (3000 Ci/mmol) was also used in the following 10-µL PCR reactions to generate a more accurate marker: 1µL of end-labeled primer, 0.5 µL of Therminator DNA polymerase, 50 nM dNTPs, 1.9 µM acyGTP or acyCTP, and 300-600 ng of template DNA (plasmid containing the *fmtA* promoter). The cycling program was: denaturation at 95 °C for 2 min; 30 cycles of 95 °C for 20 s, 55 °C for 30 s, and 72 °C for 20 s; and a final extension step at 72 °C for 5 min (primer-extension protocol modified from Harraqhy et al. 2005).

4.2.3 Determination of the TSS of *fmtA* in the *fmtA* complementary strain

4.2.3.1 Single-site mutation of pMK4 containing *fmtA* and its promoter

The predicted TSSs G-157, T-156, A-53, and A-52 were mutated (G to T, T to G, and A to C, respectively) in pMK4 containing *fmtA* and its promoter region using the QuikChange™ Site-Directed Mutagenesis Kit (Stratagene).

Primers containing targeted mutations were used to PCR-amplify pMK4 containing the *fmtA* gene and its promoter region (Table 4.1). The plasmids were digested with DpnI and then transformed by heat shock into NovaBlue competent cells that were grown on LB plates containing 50 µg/mL ampicillin. Mutation was confirmed by plasmid sequencing. The plasmids containing the expected mutated sites were then transformed into the RN4220 Δ*fmtA* strain by electroporation. Colonies were picked from TSB plates supplied with 20 µg/mL chloramphenicol, and the mutations were confirmed by plasmid sequencing.

Table 4.1 Primers used to generate mutations in pMK4 containing the *fmtA* gene and its promoter region (-450 to -1).

Primer	Primer sequence	Mutation site
DirFmtAG342T	5'-AGGTATAATTAATTTTTTGTATAGATAACAT	-157G/T
RevFmtAG342T	5'-ATGTTATCTATACAAAAAAATTAATTATACCT	
FmtA T+1G Dir	5' -GGTATAATTAATTTTGGTGTATAGATAACAT	-156T/G

FmtA T+1G Rev	5’ - ATGTTATCTATACACCAAAATTAATT ATACCT	
DirPfmtAA446C	5’- GGCATCTAGGTTCACATTTTTAACG ATTT	-53A/C
RevPfmtAA446C	5’- AAATCGTTAAAAATGTGAACCTAGA TGCC	
DirFmtAA447C	5’- GGCATCTAGGTTCAACTTTTTAACG ATTT	-52A/C
RevFmtAA447C	5’- AAATCGTTAAAAAGTTGAACCTAG ATGCC	
DirG342-10D	5’ -TCCCCCGGGATTTTGTTGTATAGAT AAC	Deletion of the -10 region of -157G
RevG342-10D	5’ - TCCCCCGGGCTTATCACTTTGTATA AAT	
RevG304-10del	5’ - GCCTTTAAATTTTTTAAGAC	Deletion of the -10 region of -195G
DirG304-10del	5’ - TCGAGTGATTTATACAAAGT	

4.2.3.2 Deletion/replacement of the -10 regions of predicted TSSs in pMK4 containing *fmtA* and its promoter

The -10 region (TATAAT, upstream from -170T to -165T) (Figure 1.2) of the predicted TSS -157G was deleted from pMK4 containing fmtA and its promoter. And the -10 region of -195G (TAATAT, upstream from -207T to -202T) was deleted from the above plasmid. Primers used are listed in Table 4.1.

PCR-amplified plasmids were digested with DpnI and then gel-extracted. An equal volume of the End conversion buffer provided with the pSTBlue-1 vector was added, and the solution was incubated at 22 °C for 15 min. One microliter of T4 DNA ligase was added and incubated at 22 °C for 20 min. Ligated plasmids were transformed by heat shock (42 °C, 2 min) into NovaBlue competent cells that were grown on LB plates containing 50 μg/mL ampicillin. Mutation was confirmed by plasmid sequencing. The plasmids containing the expected mutated sites were then transformed into the RN4220 Δ*fmtA* strain by electroporation. Colonies were picked from TSB plates supplied with 20 μg/mL chloramphenicol, and the mutations were confirmed by plasmid sequencing.

4.3 Results and Discussion

4.3.1 Determination of the TSS of *fmtA*

Adapters (provided with the FirstChoice® RLM-RACE Kit) were attached to the 5' ends of the transcripts of *fmtA* in RN4220, and PCR reactions were performed to identify the DNA fragments capable of being amplified with specific primers. Two bands with the expected size were observed on an agarose gel (Figure 4.2). Each band was isolated and sequenced, and three potential TSSs were found: -157G, -53A, and -52A.

Four single-nucleotide mutants in these three putative TSSs, together with the putative TSS, -156T, were generated to test the effect of *fmtA* in the *fmtA* complementary strain on transcription level (Figure 4.3). -156T was the previously predicted TSS (Zhao

et al. 2012). The *fmtA* complementary strain and the four mutants were referred to as: RN^{fmtA-}(*fmtA*::pMK4), RN^{fmtA-}(*fmtA*$^{-157G/T}$::pMK4), RN^{fmtA-}(*fmtA*$^{-53A/C}$::pMK4), RN^{fmtA-}(*fmtA*$^{-52A/C}$::pMK4), and RN^{fmtA-}(*fmtA*$^{-156T/G}$::pMK4), respectively.

The -10 region of each putative TSS is located about 10 nucleotides upstream of the TSS and is essential for the recognition and binding of RNA polymerase. Both -157G and -156A shared the same -10 region (TATAAT, upstream from -170T to -165T), while the -10 region of -53A and -52A lacked a common feature of the -10 regions in bacteria: a high-T/A content. The -10 region of -157G was thus deleted in the *fmtA* complementary strain, which was then referred to as RN^{fmtA-}(*fmtA*$^{-157G\text{-}10del}$::pMK4). Here, the region from -171G to -163A (9bp long) was replaced by CCCGGGGGATCCCCCGGG (18bp long).

A mutation at -157G or the deletion of its -10 region caused a significant decrease (~0.3-fold) in the level of *fmtA* transcription without oxacillin treatment relative to the wild-type *fmtA* complementary strain, but the other mutants did not significantly affect the transcription level. After oxacillin treatment, the *fmtA* transcription levels significantly increased (more than 2-fold) in all the above strains relative to the levels in the same strains without oxacillin treatment. The oxacillin-induced *fmtA* transcription level was similar to the *fmtA* expression in the wild-type *fmtA* complementary strain without oxacillin treatment (Figure 4.3) when the -10 region of -157G was deleted.

These observations indicated that -157G is likely to be the true TSS of *fmtA* without oxacillin treatment. The *fmtA* transcription level, however, was also up-regulated when treated with oxacillin, even though -157G or its -10 region was mutated, perhaps suggesting that another TSS, or multiple TSSs, of *fmtA* was responsible for the increase upon oxacillin treatment.

4.3.2 Determination of the TSS of *fmtA* by primer extension

I tested the possibility of other TSSs for *fmtA* by primer extension. Primer extension was conducted in fmtA in the RN4220 and *fmtA* complementary strains, with and without oxacillin treatment. Two TSSs were observed on a polyacrylamide gel: -195G and -157G. -157G was consistent with the TSS identified by the FirstChoice® RLM-RACE Kit. -195G was a new potential TSS. As predicted, transcription starting from -157G was not increased by oxacillin treatment, but transcription starting from -195G was significantly increased after oxacillin treatment (Figure 4.4). The band intensity from the *fmtA* complementary strain was much higher than that from RN4220, which indicated that the complementary strains had multiple copies of pMK4 fusion plasmids.

Primer extension also provided additional evidence for previous results in this study. In the *vraR*-mutated RN4220 strain, -157G was the only TSS for *fmtA*, and no band was observed at the -195G position (Figure 4.5), suggesting that transcription starting from -195G was controlled by the VraSR two-component system upon oxacillin treatment.

fmtA had a basal level of transcription at -195G in RN4220 without oxacillin treatment, while no *fmtA* transcription products were produced by the same position in *vraR*-mutated RN4220 no matter with or without oxacillin treatment (Figure 4.4 and 4.5). This finding may indicate that VraR is the only regulatory factor responsible for the basal level of transcription starting from -195G in the absence of environmental stress.

The level of *fmtA* transcription from -195G was much lower in the *fmtA* complementary strain containing M1 in P*fmtA* than in A1-deleted P*fmtA*, both with and without oxacillin treatment. This finding suggested that M1 in the VraR binding-site A2 had a larger effect on *fmtA* transcription from -195G than did the deletion of VraR binding-site A1, in agreement with previous conclusions in this study (Figure 4.5).

No transcription products were produced in the *fmtA* complementary strain where the -10 regions for both -157G and -195G had been deleted (Figure 4.6). Bands occurred at the regular -195 and -157 positions on the same polyacrylamide gel, but these bands had been produced by the genome, not the complementary plasmid, because P*fmtA* had not been deleted from the genome when the *fmtA*-mutated RN4220 was generated. This also explained why the band intensity at position -195 increased significantly under oxacillin treatment in the *fmtA* complementary strain containing M1 (Figure 4.5).

I can conclude that *fmtA* transcription initiation occurs mainly at -157G in the absence of oxacillin treatment and is not affected by oxacillin treatment, perhaps

suggesting that neither VraR nor VraR~P have an effect on transcription starting from -157G. The transcription of *fmtA* starting from -195G maintains a basal level without oxacillin treatment, likely due to a basal level of VraR expression in the absence of environmental stress, and transcription initiation at this position is dramatically up-regulated with oxacillin treatment or in the presence of other cell-wall stressors.

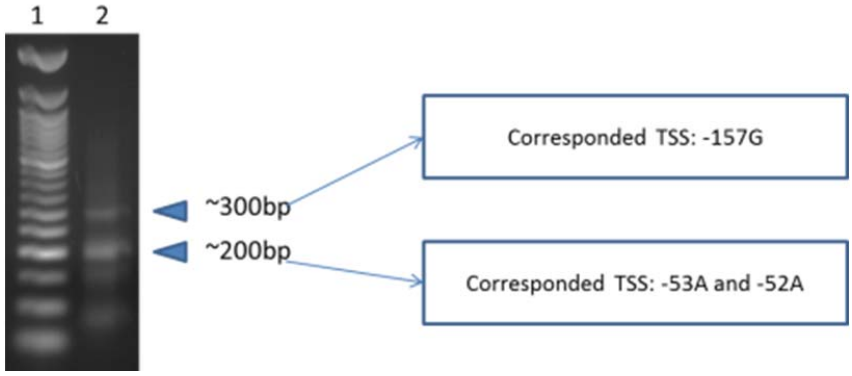

Figure 4.2 Two bands containing the potential transcription start sites of *fmtA* were inserted to pSTBlue-1 vector for sequencing. Three potential transcription start sites were identified: –157G, -53A and –52A on the *fmtA* promoter region.

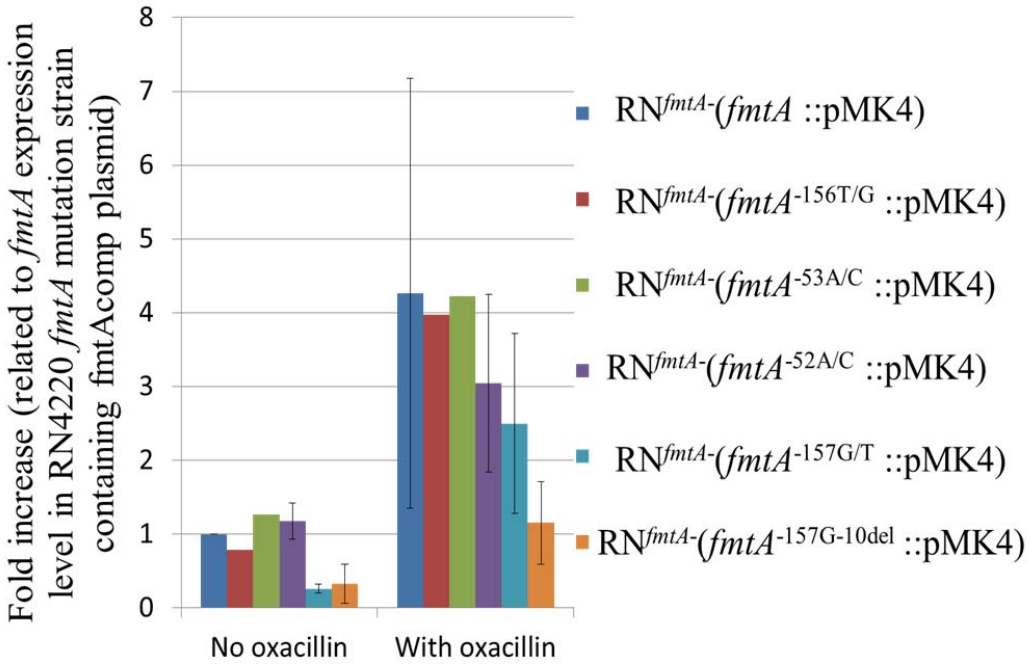

Figure 4.3 qRT-PCR results to investigate the effect on *fmtA* transcription level in *fmtA* complementary strain by single-site mutations/deletions. Single-site mutations on -156T, -53A, and -52A did not significantly change the *fmtA* expression in *fmtA* complementary strain. While, -157G/T or deletion of its -10 region significantly decreased *fmtA* expression level under non-oxacillin condition, and it was observed that, after treated by oxacillin, *fmtA* expression significantly increased in these two mutation strains.

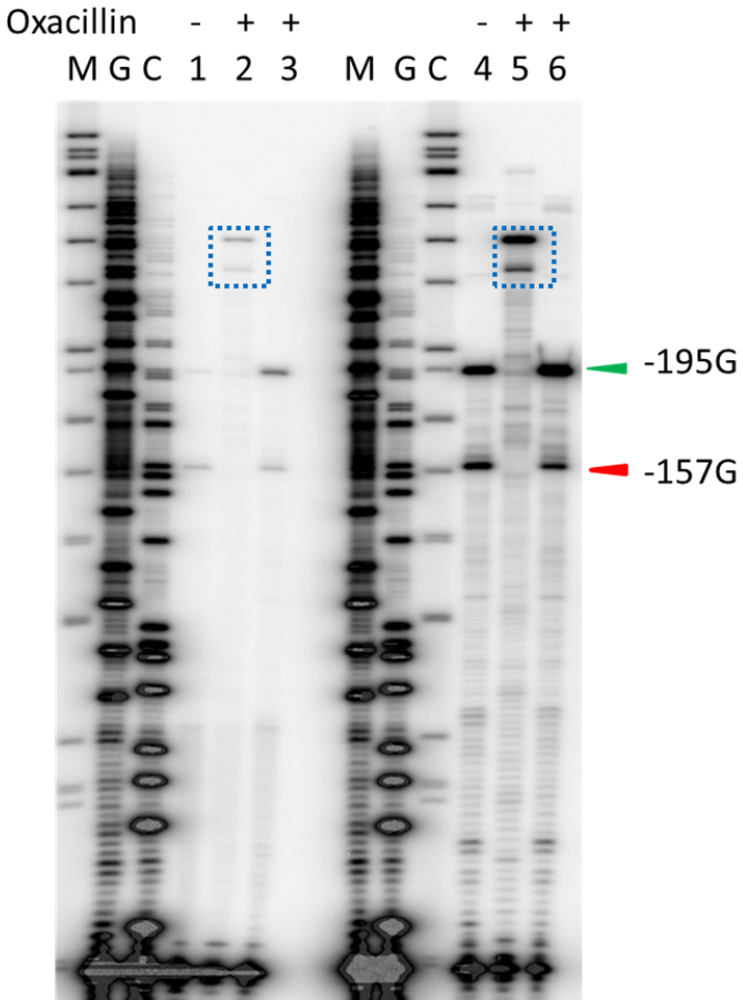

Figure 4.4 Primer extension experiments to determine the transcription start site of *fmtA*.
Lane M represents ΦX174 DNA/HinfI Dephosphorylated ladder. Lane G/C represents G/C ladder prepared by 32p-ATP labeled primer RevFmtAEx2. Lane 1/3: transcription start site of *fmtA* in RN4220 without/with oxacillin treatment. Lane 2 was similar to lane 3, except primer RevFmtAEx1 was used instead of RevFmtAEx2. Lane 4/6: transcription start site of *fmtA* in *fmtA* complementary strain without/with oxacillin treatment. Lane 5 was similar to lane 6, except primer RevFmtAEx1 was used instead of RevFmtAEx2. Two transcription start sites were observed on the gel: -157G and -195G. Lane 3 and lane 5 serve as the reference.

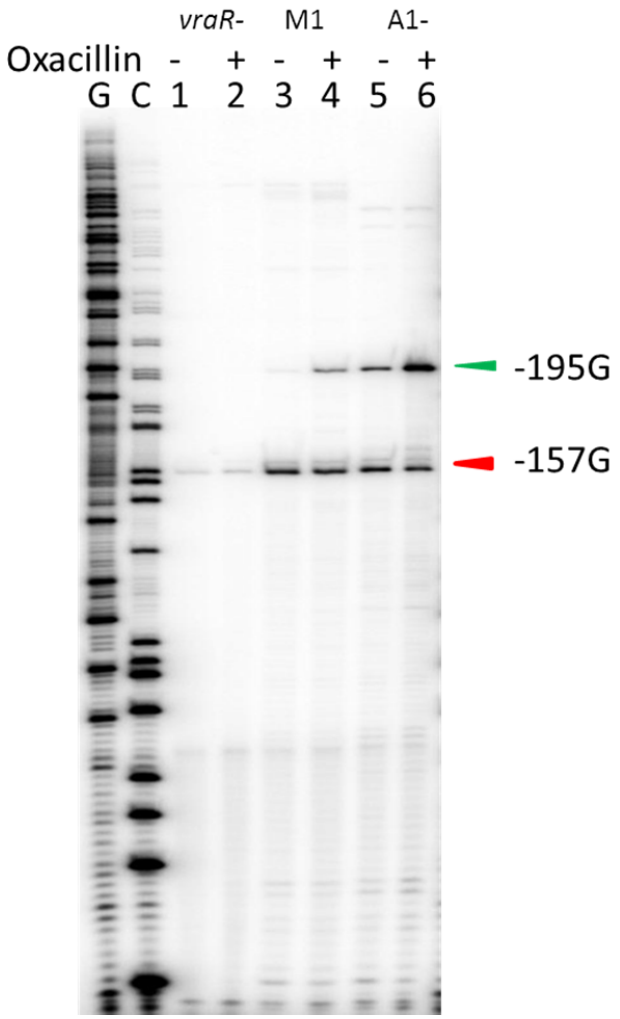

Figure 4.5 Primer extension experiments to determine the transcription start site of *fmtA* and VraR binding activity. G/C represents G/C ladder prepared by 32p-ATP labeled primer RevFmtAEx2. Lane 1/3/5: transcription start site of *fmtA* in RN4220 Δ*vraR*, *fmtA* complementary strain containing mutation M1 on P*fmtA*, and *fmtA* complementary strain containing A1-deleted P*fmtA* without oxacillin treatment. Lane 2/4/6: transcription start site of *fmtA* in RN4220 Δ(*vraR*), *fmtA* complementary strain containing M1 in the plasmid, and *fmtA* complementary strain containing A1-deleted P*fmtA* with oxacillin treatment. Positions of two putative transcription start sites -195G and -157G were indicated by green and red arrows, respectively.

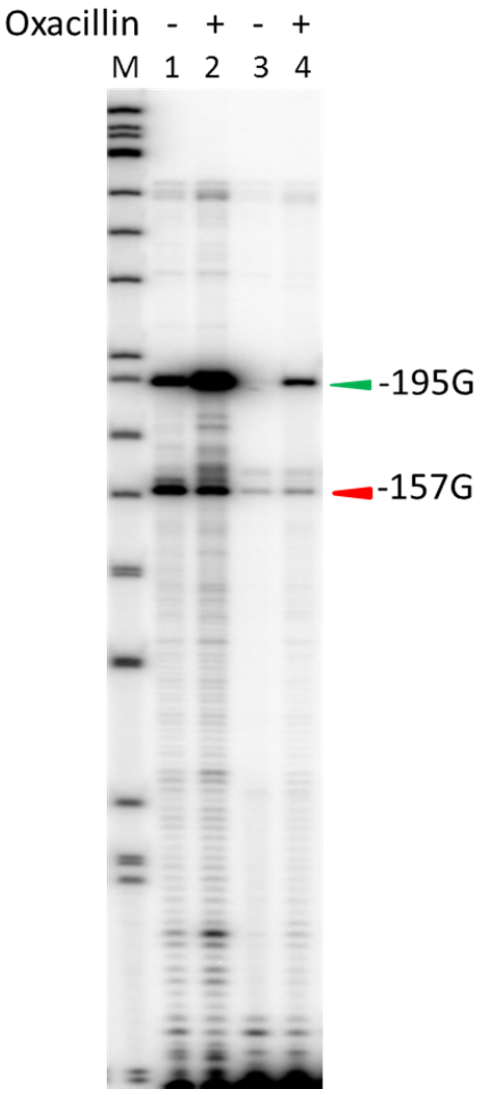

Figure 4.6 Primer extension experiments to determine the transcription start site of *fmtA*. Lane 1/3: transcription start site of *fmtA* in *fmtA* complementary strain and *fmtA* complementary strain containing deletion of -10 regions for both -195G and -157G without oxacillin treatment. Lane 2/4: transcription start site of *fmtA* in *fmtA* complementary strain and *fmtA* complementary strain containing deletion of -10 regions for both -195G and -157G with oxacillin treatment. Positions of two putative transcription start sites -195G and -157G were indicated by green and red arrows, respectively.

CHAPTER FIVE: INVESTIGATION OF VRAR BINDING ACTIVITY AT THE PROMOTERS OF *MURZ*, *SGTB*, AND *PBP2*

5.1 Introduction

More than 40 genes in *S. aureus* are considered members of the VraSR regulon and are up-regulated in the presence of vancomycin, oxacillin, and other cell-wall inhibitors (Bernal et al. 2010; Utaida et al.2003; Kuroda et al. 2003; McAleese et al. 2006; Muthaiyan et al. 2008; Sengupta et al. 2012). Of these genes, *murZ*, *pbp2*, and *sgtB* are clearly involved in the peptidoglycan biosynthesis pathway and are under the direct control by the VraSR two-component system (Sengupta et al. 2012). The *in vivo* evidence indicates that VraR is capable of binding to the promoter regions of these three genes with oxacillin induction (Sengupta et al. 2012). The positions of *murZ*, *pbp2*, and *sgtB* and their promoter regions are shown in Figure 5.1.

murZ encodes UDP-N-acetylglucosamine enolpyruvyl transferase (MurZ) (also known as UDP-N-acetylglucosamine 1-carboxylvinyl transferase 2). MurZ transfers an enolpyruvyl group from phosphoenolpyruvate to UDP-N-acetylglucosamine to form UDP-N-acetylglucosamine enolpyruvate (a precursor to UDP-N-acetylmuramate, an essential component of the cell wall), which is the first committed step in peptidoglycan (PG) biosynthesis occurring at the cytoplasmic stage (Silver 2006; Du et al. 2000). The expression of MurZ is inducible by inhibitors of PG biosynthesis (Blake et al. 2009).

MurZ is the minor of two forms of UDP-N-acetylglucosamine enolpyruvyl transferase in *S. aureus* (MurA is the major form). The mutation of *murZ* reduces the PG content of the cell wall by only 3% (Du et al. 2000; Blake et al. 2009), perhaps suggesting that *murZ* mainly compensates for damage to the cell wall when stressed.

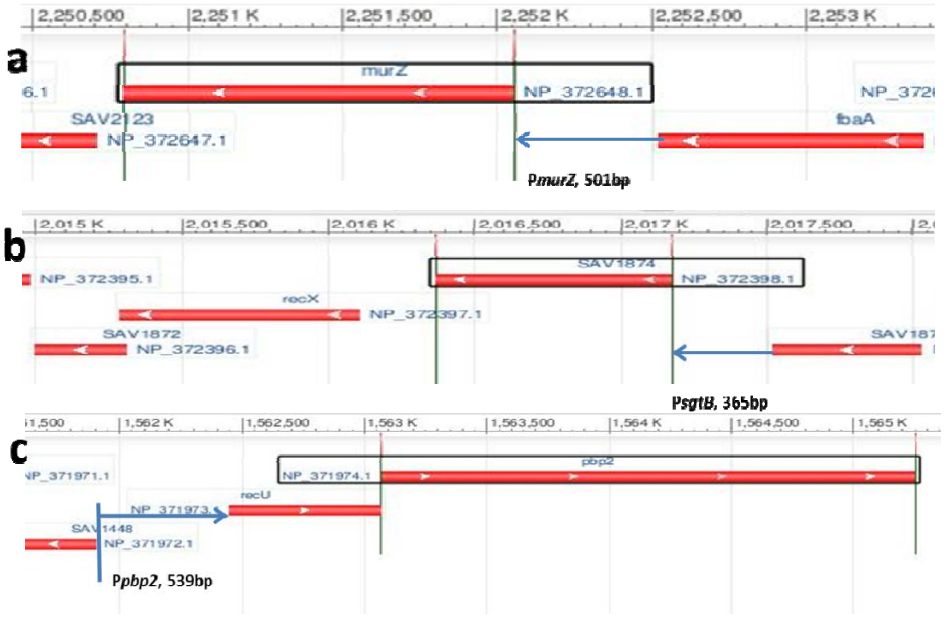

Figure 5.1 *murZ*, *sgtB* and *pbp2* genes and their promoters in the genome of *S. aureus* strain Mu50. Blue arrowed lines indicate the range of the promoters and the direction of transcription (5' – 3'). SAV1874 is the predicted *sgtB* gene.

SgtB (or MGT) is a putative monofunctional glucosyltransferase encoded by *sgtB*. The role of SgtB under cell-wall stress may become important in the final stages of peptidoglycan biosynthesis (Sengupta et al. 2012). The assembly of peptidoglycan polymers requires two types of enzymes: peptidoglycan glycosyltransferases (PGTs) and transpeptidases (TPs). PGTs catalyze the elongation of the carbohydrate chains, and TPs

catalyze cross-linking (Rebets et al. 2014; Lovering et al. 2008). *S. aureus* contains two monofunctional PGTs (SgtA and SgtB) and one bifunctional PGT (PBP2, with TP activity) (Rebets et al. 2014). Neither SgtA nor SgtB are essential in *S. aureus*, but SgtB is the only PGT that can compensate for the loss of the PGT domain in PBP2 in terms of the viability of *S. aureus* (Reed et al. 2011). PBP2, encoded by *pbp2* (also known as *pbpB*), is a native penicillin-binding protein in MRSA and the only penicillin-binding protein having an N-terminal PTG domain and a C-terminal TP domain (Pinho et al. 2001). PBP2 catalyzes the cross-linking of carbohydrate chains (Rebets et al. 2014). Its transpeptidase activity can be compensated by PBP2A, a foreign-acquired PBP with low β-lactam affinity under β-lactam stress (Pinho et al. 2001). Both the transglycosylase domain of PBP2 and the transpeptidase domain of PBP2A, however, are important for cell-wall synthesis under β-lactam stress (Pinho et al. 2001; Pinho et al. 1998). Gardete et al. (2006) reported that the level of PBP2 expression could be rapidly sensed by the VraSR two-component system and that subsequent responses were made. The double roles of PBP2 as the trigger of the VraSR two-component system and as a member of the VraSR regulon highlight the importance of fully understanding the regulatory mechanism of *pbp2*.

5.2 Materials and Methods

5.2.1 Determination of VraR binding activity at the promoters of *murZ*, *pbp2*, and sgtB by DNase I footprinting

The primer pairs in Table 5.1 were used to PCR-amplify the promoter regions of *murZ*, *pbp2*, and *sgtB*, and the amplified fragments were inserted into the pSTBlue-1 vector. Each promoter region was divided into two fragments, and each fragment was investigated by DNase I footprinting.

Table 5.1 Primers used in the PCR amplification of the promoters of *murZ*, *pbp2*, and *sgtB*. Each promoter was divided into two short fragments, Seq1 and Seq2, and VraR/VraR~P binding activity at both fragments was investigated by DNase I footprinting. The A of the translation initiation codon (ATG) is referred to as +1 for *murZ* and *sgtB*, respectively. While the A of the translation start codon of *pbp2* is +624, because *pbp2* and *recU* share the same operon and the +1 position starts from the translation start codon of recU.

Primer	Primer sequence	Amplified fragment
DirP*murZ*	5’ - ATTAAAGAGTTCGGTACTT	-501 to -1, Full P*murZ*
RevPmurZ	5’ - ATCATTTATCTCCTTTGTCC	
DirPpbp2	5’ - GAGGACGCCTCCTACATT	-539 to -1, Full P*pbp2*
RevPpbp2	5’ - AAATTTCACCACACAAGT	
DirPsgtB	5’ - GAGAAATCGTTAAACAATTAC	-365 to +2, Full P*sgtB*
RevPsgtB	5’ - ATGCGTTTGCTCCTTCTT	
DirPmurZ	5’ - ATTAAAGAGTTCGGTACTT	-501 to -252, Seq1 of P*murZ*,
RevPmurZseq1	5’ - TTTGTACGTAAACTTTTTTC	
DirPmurZseq2	5’ - TCGTAGAATTAAAACTAAAT	-251 to -1, Seq2 of P*murZ*
RevPmuZ	5’ - ATCATTTATCTCCTTTGTCC	
DirPpbp2	5’ - GAGGACGCCTCCTACATT	-539 to -270,

RevPpbp2seq1	5’ - ATCAGTAATTTTTATTTTTGAG	Seq1 of P*pbp2*
DirPpbp2seq2	5’ - CATGATTTGACTTTTATAAC	-269 to -1, Seq2 of P*pbp2*
RevPpbp2	5’ - AAATTTCACCACACAAGT	
DirPsgtB	5’ - GAGAAATCGTTAAACAATTAC	-365 to -203, Seq1 of P*sgtB*
RevPsgtBseq1	5’ - TTGTAAAATAAAAGACCATC	
DirPsgtBseq2	5’ - AATATAACAATATTTGGCATG	-202 to +2, Seq1 of P*sgtB*
RevPsgtB	5’ - ATGCGTTTGCTCCTTCTT	

The primers pairs were used for the PCR amplification of seq1 of P*murZ*, seq2 of P*murZ*, seq1 of P*pbp2*, seq2 of P*pbp2*, seq1 of P*sgtB*, and seq2 of P*sgtB*. All amplified DNA fragments were purified using the QIAquick Gel Extraction Kit (Qiagen) and used as PCR templates in the DNase I footprinting assays. The 5’-end of the primer of interest (forward or reverse) was labeled with [γ-^{32}P] ATP (3000 Ci/mmol) using 20 U of T4 polynucleotide kinase (NEB) and used to amplify seq1-3 in a 20-μL reaction. Binding reactions were prepared in binding buffer (10 mM Tris-base, pH 7.5, 50 mM KCl, and 1 mM DTT) supplemented with 5 mM $MgCl_2$, 0.05% herring sperm DNA, and 2.5% glycerol. The end-labeled DNA (6-8 ng) was mixed with VraR/VraR~P at concentrations ranging from 0 to 40 μM. The binding reactions were incubated for 30 min at room temperature and then digested with DNase I (0.024 U/reaction) for 2 min. The digestion reactions were stopped by adding 50 μL of DNase I stop solution (1% SDS, 0.2 M NaCl, and 20 mM EDTA, pH 8.0). Digested DNA samples were extracted by phenol-chloroform and then precipitated with ethanol. Purified DNA was resuspended in loading dye containing 10 mM formamide, 1 mg/mL bromophenol blue, and 1 mg/mL xylene cyanol,

incubated at 95 °C for 5 min, and electrophoresed on an 8% polyacrylamide gel containing 7 M urea. The dried gels were exposed to a phosphor screen for 18-24 h and scanned using a Typhoon Trio+ variable-mode imager (GE HealthCare). The C and G sequencing reactions for these experiments were performed in 10-µL PCR reactions containing 1 µL of end-labeled primer, 0.5 µL of Therminator DNA polymerase, 50 nM dNTPs, 1.9 µM acyGTP or acyCTP, and 25 ng of template DNA (gel-purified seq1-3).

5.2.2 Determination of the TSSs of *murZ*, *pbp2*, and *sgtB* by primer extension

The primers in Table 5.2 were used in primer-extension experiments to investigate the TSSs of *murZ*, *pbp2*, and *sgtB*. Total RNA was isolated, and 100 µg were dissolved in 60 µL of hybridization buffer (40 mM PIPES, pH 6.4, 1 mM EDTA, and 0.4 M NaCL, 80% (v/v) formamide) at 65 °C. For each reaction, 0.5 pmol of primer labeled with [γ-^{32}P]ATP (3000 Ci/mmol) were added, and the solutions were incubated at 95 °C for 5 min for denaturation and at 45 °C for 4 h for annealing. The samples were precipitated with ethanol and dissolved in 9 µL of distilled water, and the following components were added: 3 µL 5xAMV-RT buffer, 0.75 µL of RNasin, 0.75 µL of dNTPs (20 mM), and 0.75 µL of D-actinomycin (4 mg/mL). After incubation at 42 °C for 2 min, 1.3 µL (13 U) of AMV-RT were added, and the mixture was incubated at 42 °C for 2 h. The reaction was terminated by adding 25 µL of stop buffer (100 µg/mL RNase A and 30 µg/mL herring sperm DNA in TE buffer, pH 8.0) and then incubated at 37 °C for 30 min. After

precipitation with ethanol, the samples were dissolved in 7 μL of loading buffer (10 mM NaOH, 1 mM EDTA, 0.05% xylene cyanol and bromophenol blue, and 80% formamide) and were electrophoresed on an 8% polyacrylamide sequencing gel. The dried gels were exposed to a phosphor screen for 18-24 h and scanned using a Typhoon Trio+ variable-mode imager (GE HealthCare). A phiX 174 DNA/HinfI dephosphorylated marker labeled with [γ-^{32}P]ATP (3000 Ci/mmol) was used to indicate the position of the RNA transcription products of *fmtA*. The primer RevFmtAEx2 labeled with [γ-^{32}P]ATP (3000 Ci/mmol) was also used in the 10-μL PCR reaction below to generate a more accurate marker: 1 μL of end-labeled primer, 0.5 μL of Therminator DNA polymerase, 50 nM dNTPs, 1.9 μM acyGTP or acyCTP, and 300-600 ng of template DNA (plasmid containing the *fmtA* promoter). The cycling program was: initial denaturation at 95 °C for 2 min; 30 cycles of 95 °C for 20 s, 55 °C for 30 s, and 72 °C for 20 s; and a final extension step at 72 °C for 5 min.

Table 5.2 Primers used in the primer-extension experiments to investigate the TSSs of *murZ*, *pbp2*, and *sgtB*.

Primer	Primer sequence	Target gene
RevMurZex1	5’ - TTAGTGTGCGTCCACCTC	TSS of *murZ*
RevSgtBex1	5’ - GGTTTGCCAACTGGTTGAT	TSS of *sgtB*
RevPbp2ex1	5’ - GATAAAACGTATTTGAATGTTCG	TSS of *pbp2*

5.3 Results and Discussion

5.3.1 Investigation of VraR binding sites in P*murZ*, P*sgtB*, and P*pbp2*

The DNase I footprinting assays identified a VraR/VraR~P-protected region on Seq2 of P*murZ* on both the top and bottom strands: 5' - GTTGAataaTCAGACTttAGACCATGGTCAAGTGGGGAAGAACAGCA (top-strand sequence) (Figure 5.2a and 5.2b). The underlined sequence was protected by VraR~P only. Two putative VraR binding motifs (highlighted in red and green) were found in this site. They were highly conserved with the VraR binding motifs identified in the *vraSR* promoter (Belcheva et al. 2009) and the *fmtA* promoter in the present study.

A VraR/VraR~P-protected region was identified on Seq2 of P*sgtB* on both the top and bottom strands: 5' - GTAAGTATGATGGCGTATACGATTGTAAGCCCTTGGACTGATTTTCCCAAAAAG TGTAGCC (top-strand sequence). The underlined sequence was protected by VraR~P only (Figure 5.2c and 5.2d). No highly conserved VraR binding motifs were found.

Only two regions protected by VraR~P were found on Seq1 and Seq2 of Ppbp2. The Seq1 region was 5'-CGATGAAAATACTTTTAATCTAATAAAATCATTTAAATCAAATACACCTCTGC TGATTAA (top-strand sequence) on both the top and bottom strands (Figure 5.2e and 5.2f). The Seq2 region was

5’-ATCACGTTAAAATAAGCTTTGGTGTATTGTGTCTTTCGCATTTATACTAATTTA AGTTTGGTGTTTC (top-strand sequence) on both the top and bottom strands (Figure 5.2g and 5.2h). No highly conserved VraR binding motifs were found in these two regions.

5.3.2 The TSSs of *murZ*, *sgtB*, and *pbp2*

Primer extension assays were performed to determine the TSSs in *murZ*, *sgtB*, and *pbp2* in RN4220, both with and without oxacillin treatment (Figure 5.3).

Two potential TSSs of *murZ* were identified (Appendix Figure 2a). One (-146G) had an increased band intensity upon oxacillin treatment, and the intensity of the other band (-42A) changed little (Figure 5.3). The conserved VraR binding motifs in P*murZ* may indicate that *murZ* has a similar VraR binding activity at its promoter region and a similar mechanism of transcription initiation (one of the two TSSs (-146G) being responsible for the reaction to oxacillin treatment, and the other (-40G) maintaining the basal level of gene transcription).

Only one TSS for *sgtB* (-38G) was found (Appendix Figure 2b), and the transcription level increased with oxacillin treatment (Figure 5.3).

At least four TSSs (-105T, -30G, +87T, and +89G) of *pbp2* were identified (Appendix Figure 2c), three of which (-30G, +87T, and +89G) had significantly increased levels of transcription with oxacillin treatment (Figure 5.3). The *recU* gene is located

upstream of *pbp2* in the same operon. Nucleotide position +1 refers to the A of the translation start codon (ATG) of *recU*, and the A of the translation start codon (ATG) of *pbp2* is located at +624. *recU* and *pbp2* share a 4-bp overlap, ATGA, which includes the translation stop codon TGA of *recU* and the translation start codon ATG of *pbp2*. Three TSSs for *pbp2* have been identified in the *S. aureus* COL strain: -105T, -30G, and +551A (Pinho et al. 1998). Two of these, -105T and -30G, were also identified in our study. I did not find the TSS at +551A identified by Pinho et al. (1998) because it was outside the range of the primer used. +87T and +89G were not observed by Pinho et al. (1998), perhaps because the transcription products starting from these two sites were due to induction by oxacillin. More TSSs for *pbp2* may be identified in the *recU* gene upon oxacillin treatment.

The identification of the precise nucleotides for each potential TSS was difficult due to the size of the gels in the primer-extension assays and the limitation of the phiX 174 DNA/HinfI dephosphorylated ladder. Primers closer to the currently identified TSSs for each gene should be designed to verify our results.

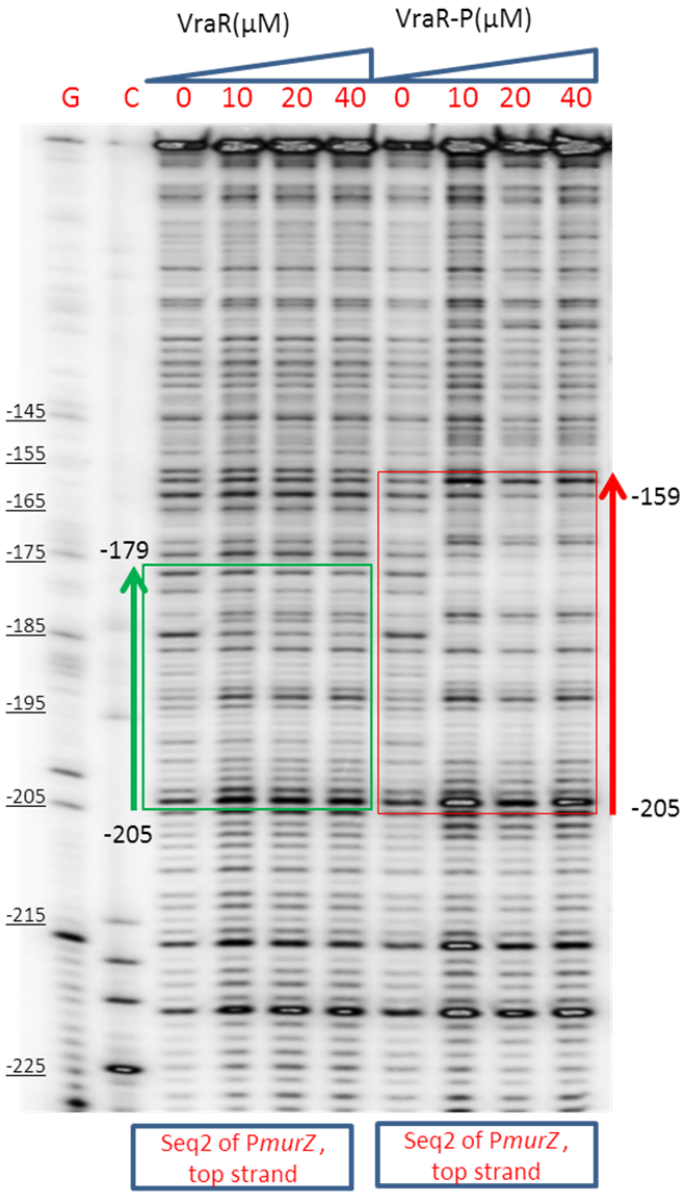

Figure 5.2a Investigation of VraR/VraR~P binding activity on the top strand of P*murZ* Seq2 by the DNase I footprinting assay. The region protected by unphosphorylated VraR is indicated by the green box and arrowed line. VraR~P protected sequence is indicated by the red box and arrowed line. Arrow direction represents sequence direction from 5' to 3' on the top strand. Numbers represent the start and end nucleotides of the protected region in the top strand of P*murZ*.

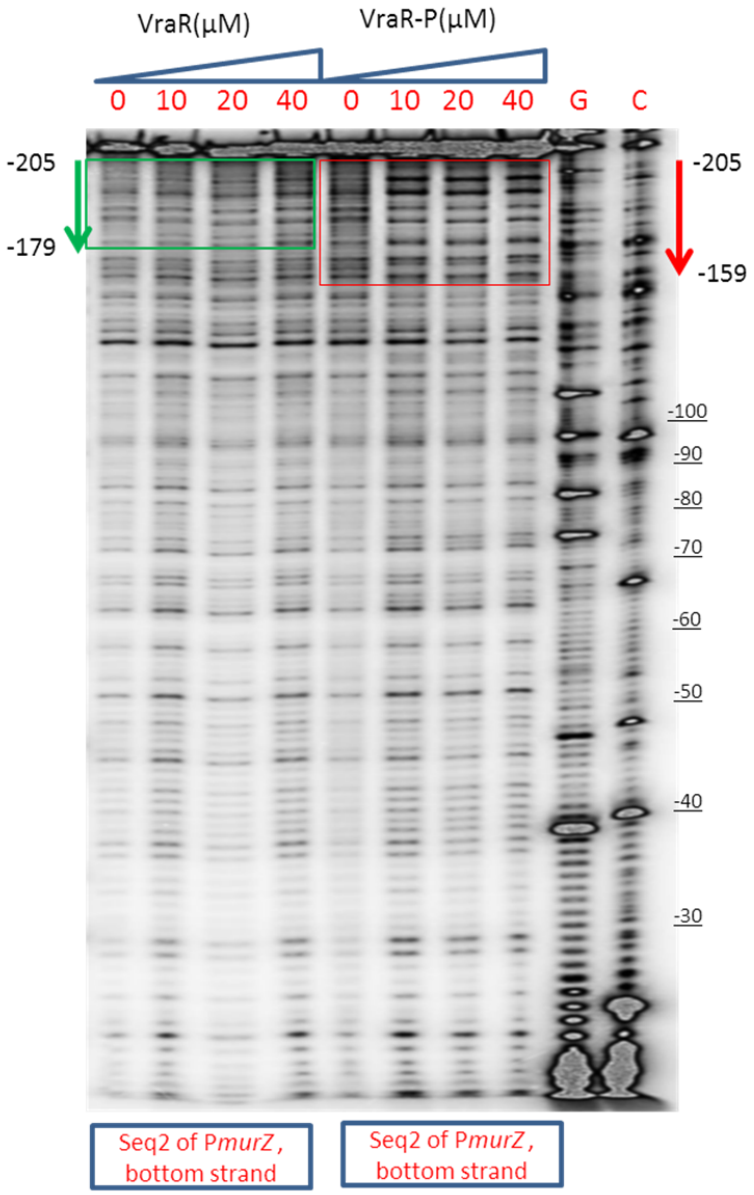

Figure 5.2b Investigation of VraR/VraR~P binding activity on the bottom strand of P*murZ* Seq2 by the DNase I footprinting assay. The region protected by unphosphorylated VraR is indicated by the green box and arrowed line. VraR~P protected sequence is indicated by the red box and arrowed line. Arrow direction represents sequence direction from 5' to 3' on the top strand. Numbers represent the start and end nucleotides of the protected region in the top strand of P*murZ*.

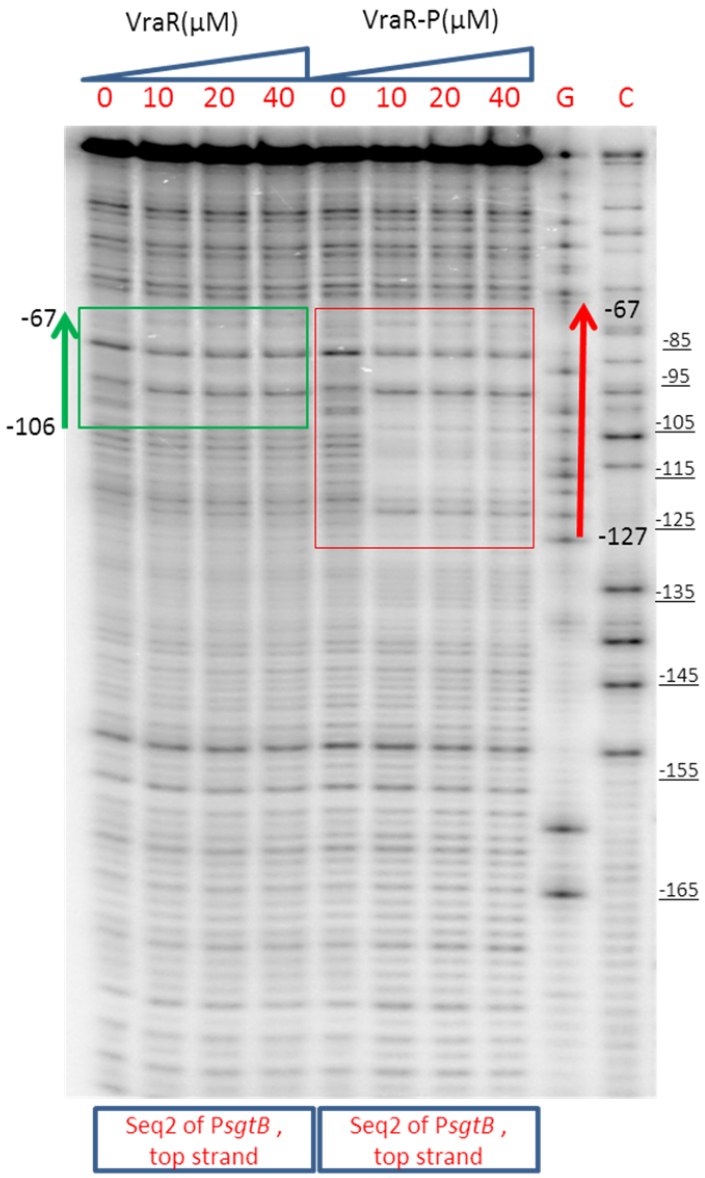

Figure 5.2c Investigation of VraR/VraR~P binding activity on the top strand of P*sgtB* Seq2 by DNase I footprinting assay. The region protected by unphosphorylated VraR is indicated by the green box and arrowed line. VraR~P protected sequence is indicated by thered box and arrowed line. Arrow direction represents sequence direction from 5' to 3' on the top strand. Numbers represent the start and end nucleotides of the protected region in the top strand of P*sgtB*.

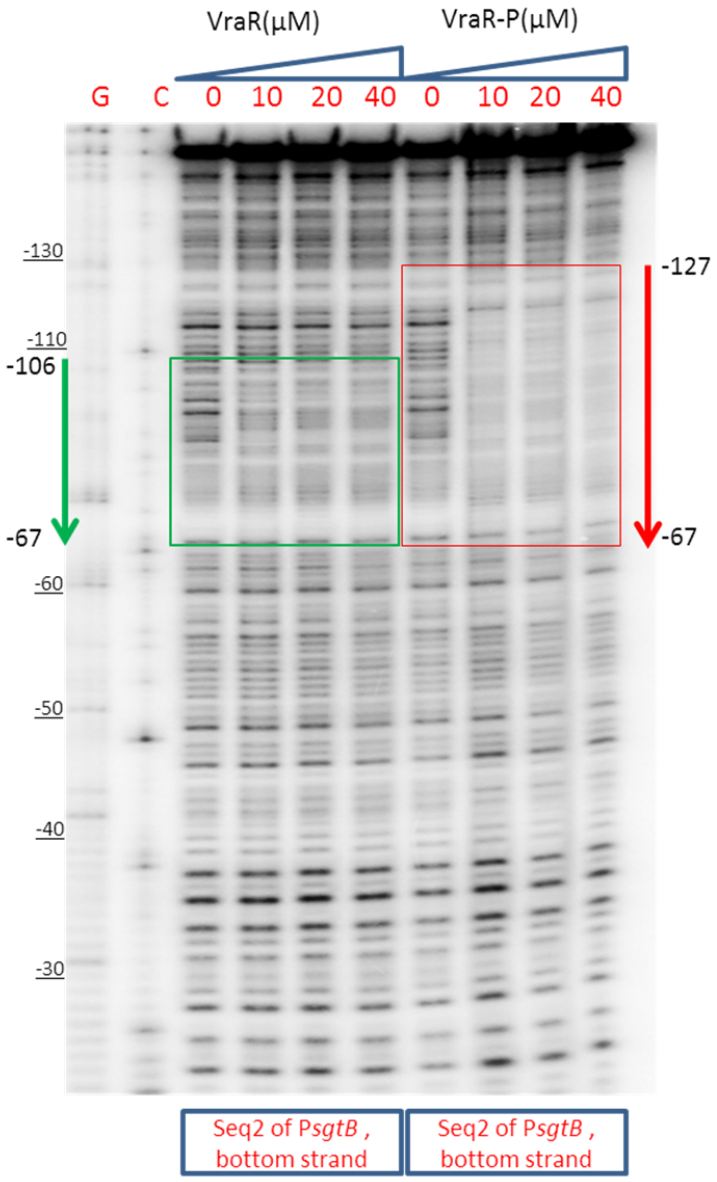

Figure 5.2d Investigation of VraR/VraR~P binding activity on the bottom strand of P*sgtB* Seq2 by DNase I footprinting assay. The region protected by unphosphorylated VraR is indicated by the green box and arrowed line. VraR~P protected sequence is indicated by the red box and arrowed line. Arrow direction represents sequence direction from 5' to 3' on the top strand. Numbers represent the start and end nucleotides of the protected region in the top strand of P*sgtB*.

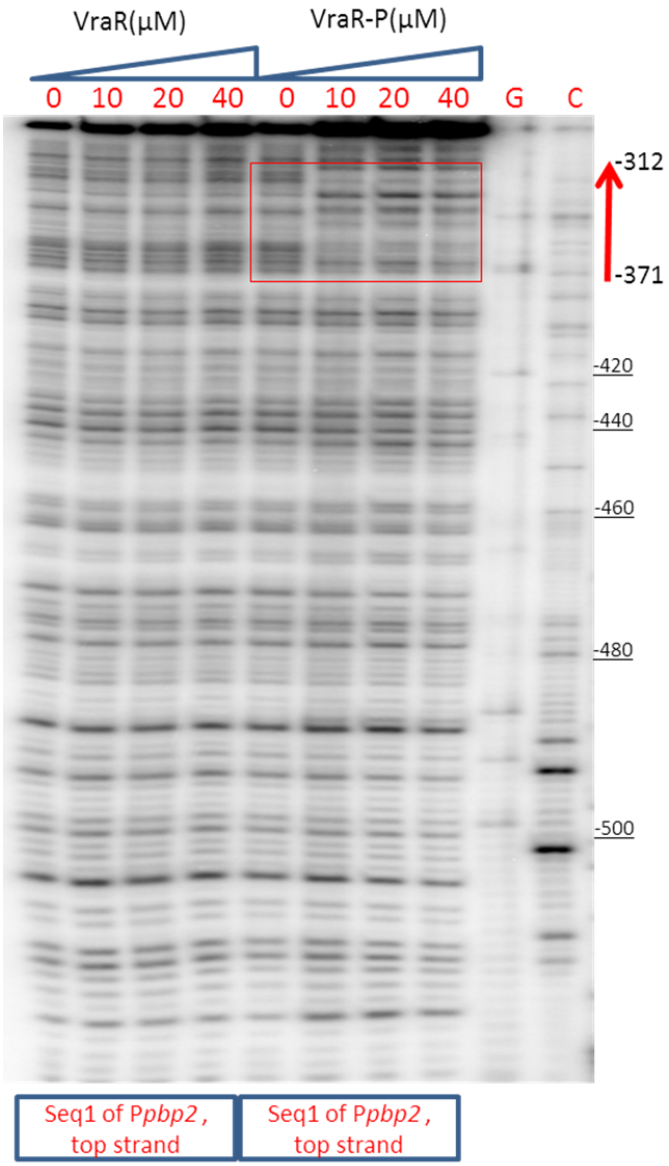

Figure 5.2e Investigation of VraR/VraR~P binding activity on the top strand of P*pbp2* Seq1 by DNase I footprinting assay. VraR~P protected region is indicated by the red box and arrowed line. Arrow direction represents sequence direction from 5' to 3' on the top strand. Numbers represent the start and end nucleotides of the protected region in the top strand of P*pbp2*.

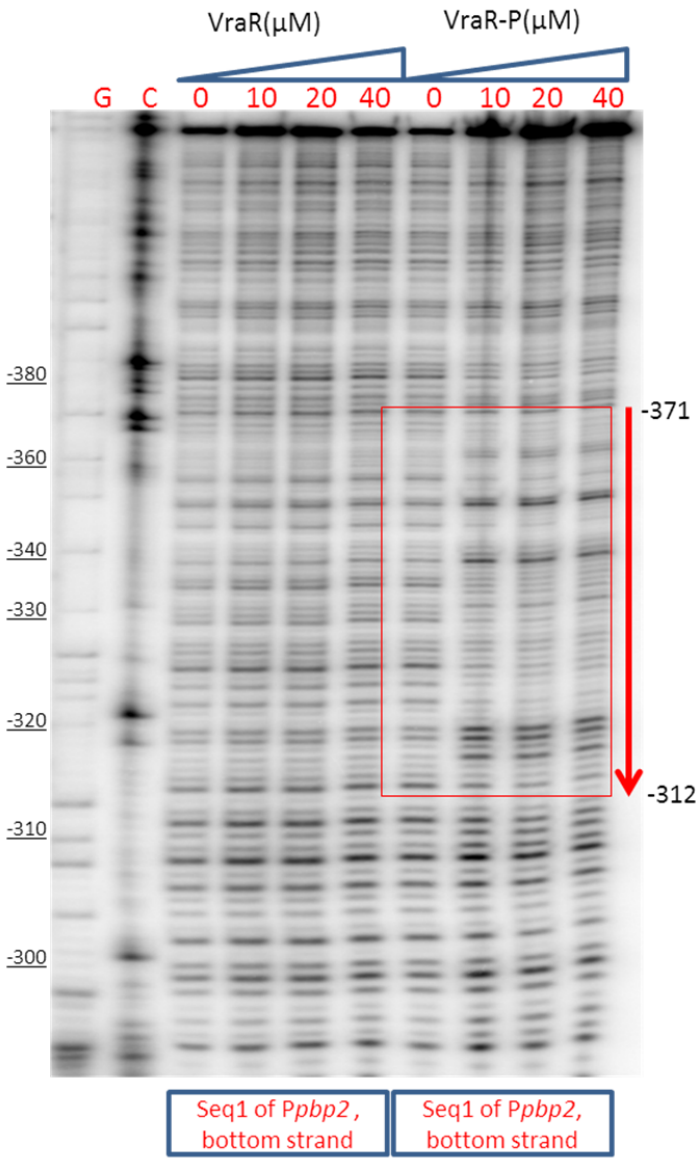

Figure 5.2f Investigation of VraR/VraR~P binding activity on the bottom strand of P*pbp2* Seq1 by DNase I footprinting assay. VraR~P protected region is indicated by the red box and arrowed line. Arrow direction represents sequence direction from 5' to 3' on the top strand. Numbers represent the start and end nucleotides of the protected region in the top strand of P*pbp2*.

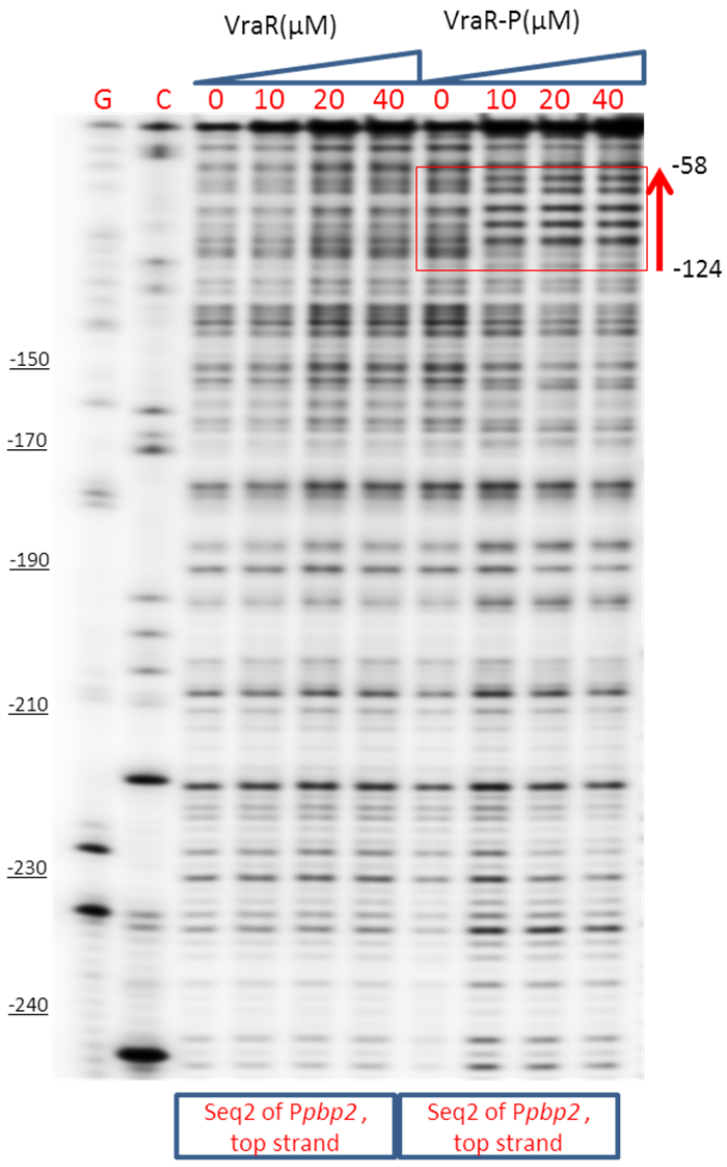

Figure 5.2g Investigation of VraR/VraR~P binding activity on the top strand of P*pbp2* Seq2 by DNase I footprinting assay. VraR~P protected region is indicated by the red box and arrowed line. Arrow direction represents sequence direction from 5' to 3' on the top strand. Numbers represent the start and end nucleotides of the protected region in the top strand of P*pbp2*.

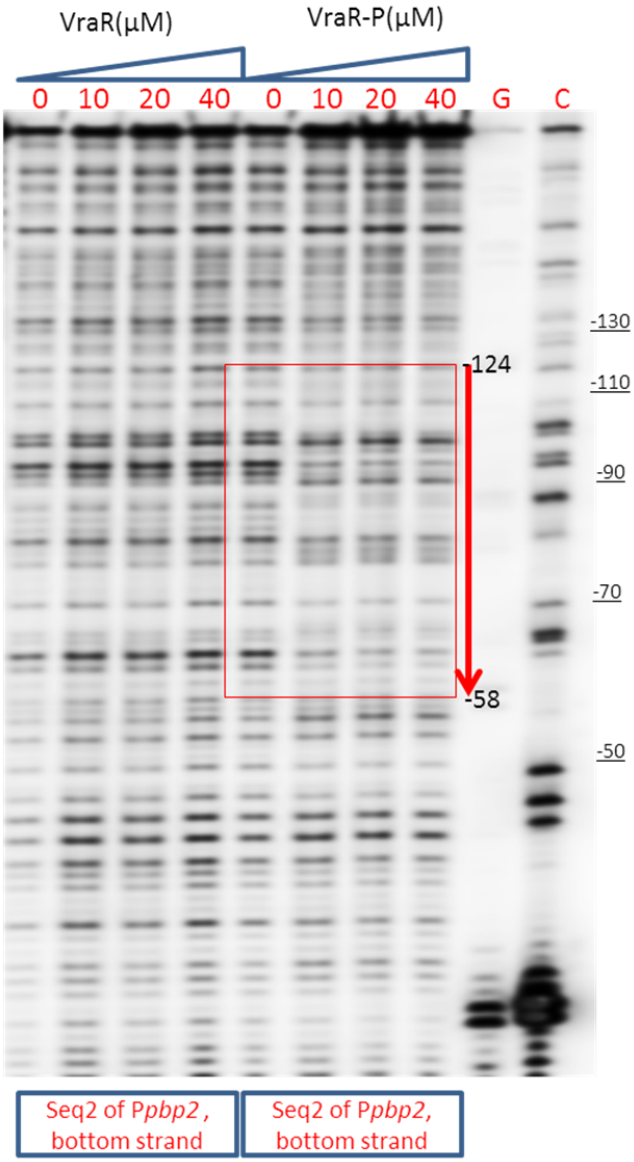

Figure 5.2h Investigation of VraR/VraR~P binding activity on the bottom strand of P*pbp2* Seq2 by DNase I footprinting assay. VraR~P protected region is indicated by the red box and arrowed line. Arrow direction represents sequence direction from 5' to 3' on the top strand. Numbers represent the start and end nucleotides of the protected region in the top strand of P*pbp2*.

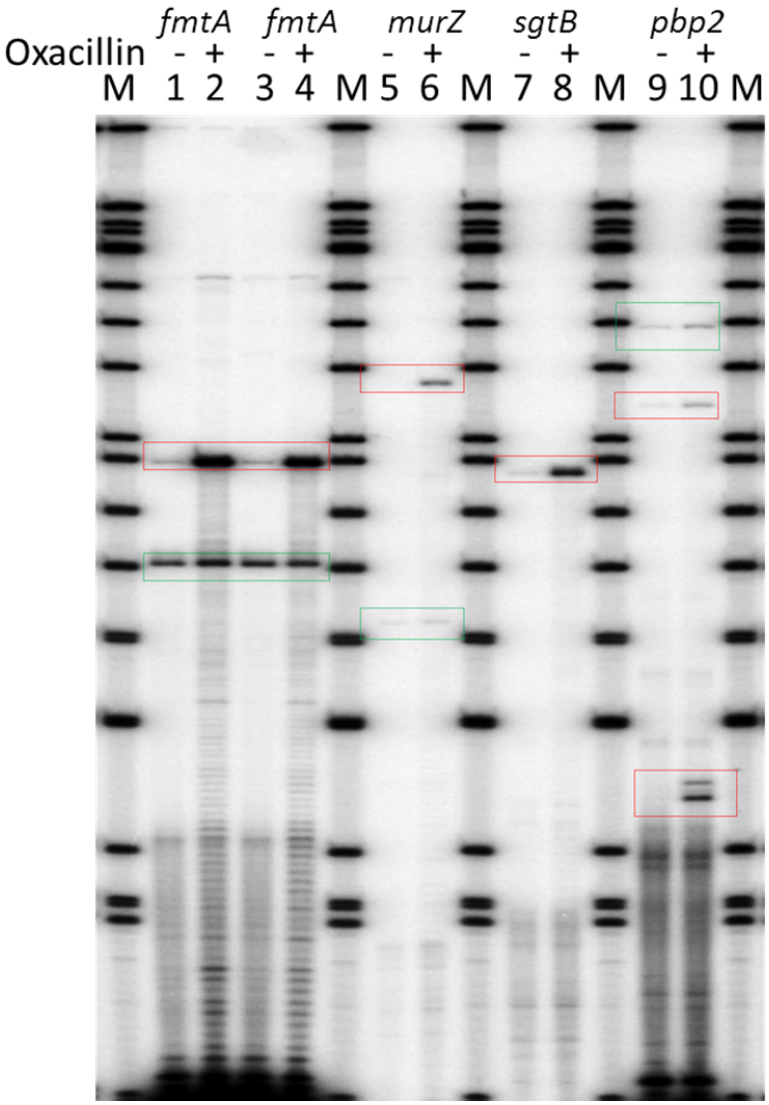

Figure 5.3 Primer extension experiments to determine the transcription start sites of *murZ, sgtB* and *pbp2*. M represents ΦX174 DNA/HinfI Dephosphorylated ladder. Lane 1, 5. 7, 9: transcription start sites of *fmtA, murZ, sgtB* and *pbp2* in RN4220 without oxacillin presence. Lane 2, 6, 8, 10: transcription start sites of *fmtA, murZ, sgtB* and *pbp2* in RN4220 in the presence of oxacillin. Lane 3/4: transcription start site of *fmtA* in PC1839 (RN4220 *sarA* mutation strain) without/with oxacillin. Red/green boxes indicate potential transcription start sites which are/not up-regulated in the presence of oxacillin.

CHAPTER SIX: CONCLUSIONS AND PERSPECTIVES

Previous work has shown that the VraSR two-component system is able to sense damage on the cell wall and to coordinate a rapid response, including the upregulation of the transcription of a set of genes, to enhance the resistance to peptidoglycan inhibitors, especially to relatively low concentrations of antibacterial agents (Kawada-Matsuo 2011;Gardete et al. 2006; Kuroda et al. 2003). Kuroda and co-workers (2003) discovered the *vraSR* operon by profiling genome-wide levels of transcription in a *vraSR*-null *S. aureus* strain, KVR. Sengupta and co-workers (2012) further identified genes under the direct regulation of VraR by its binding to their promoter regions. Belcheva and co-workers (2009) identified the regulatory mechanism of the binding of VraR to the *vraSR* promoter. They observed that the *vraSR* promoter harbored three distinct VraR binding sites with variable sequence features and affinities for VraR or phosphorylated VraR. The evidence suggests that the direct binding of VraR to promoters may be a general mechanism for regulating the transcription of related genes.

I investigated the VraR binding activity on the promoter of *fmtA*. *In vitro* data indicated two VraR binding sites on the *fmtA* promoter: A1 and A2. The A2 site showed a higher affinity than the A1 site with VraR and phosphorylated VraR in both EMSAs and DNase I footprinting assays. The mutation of one or two essential nucleotides in the A2 site effectively disrupted its interaction with VraR/phosphorylated VraR, while mutations

in the A1 site had no obvious effect. Mutations in the A1 site consistently had no effect on *fmtA* promoter strength *in vivo* in *S. aureus* RN4220 *lux* fusion strains, while mutation of the A2 site caused the loss of promoter strength under oxacillin treatment, suggesting that the A2 site may be the major VraR binding site in the *fmtA* promoter.

Deleting the entire A1 site from the *fmtA* promoter had no effect on its promoter strength, and deleting the A1 site from the *fmtA* complementary strain did not change the transcriptional level of *fmtA*, as determined by qRT-PCR. These results suggest that the A1 site is not required for the regulation of *fmtA* transcription under oxacillin stress.

The A2 site ($^{-241}$ACTttAGTaTGAtgTCt^{-225}) is similar to the R1 VraR binding site in the *vraSR* promoter and includes two putative VraR binding motifs, which are also conserved with the previously identified VraR binding motifs R1a (ACTaaAGT) and R1b (TGAacaTCA) in the *vraSR* promoter (Belcheva et al. 2009). These two motifs are separated by a single A in both promoters. Our research group has observed that mutating either of these two motifs in the A2 site could eliminate the upregulation of *fmtA* transcription under oxacillin stress (unpublished). I found that the insertion of an additional A between these two motifs had the same effect. These findings suggest that unphosphorylated VraR might not be able to bind to these two motifs unless they are dimerized.

Two transcription start sites, -157G and -195G, unlike in the *vraSR* operon, were identified in the *fmtA* promoter by primer extension and RLM-RACE. Previous extension assays also provided further evidence of VraR binding activity and of its binding mechanism on the *fmtA* promoter. Under non-stress conditions, -157G appears to be the major transcription start site, and the transcription is independent of oxacillin treatment. Transcription starting from -195G maintained a basal level in the absence of stress and corresponded to the upregulation of *fmtA* under oxacillin treatment. The *vraR*-mutated strain of RN4220 continued to express *fmtA* transcripts starting from -157G regardless of the presence of oxacillin, but the *fmtA* transcripts starting from -195G were not upregulated by oxacillin treatment, suggesting that oxacillin-induced VraR or phosphorylated VraR was responsible for the transcription initiated at -195G.

murZ, *sgtB* and *pbp2* encode essential enzymes involved in various steps of the biosynthesis of peptidoglycan. They also belong to the VraSR regulon family, and VraR modulates their transcription by directly binding to their promoters (Kuroda etal. 2003; Sengupta et al. 2012). The VraR/VraR~P-protected sequences in the DNase I footprinting assays have been identified in these promoters. A putative VraR binding region conserved with the VraR binding site A2 in the *fmtA* promoter and with the R1 binding site in the *vraSR* promoter has been observed in the *murZ* promoter. No similarly conserved regions,

however, have been found in the other two promoters, perhaps suggesting that VraR recognizes other types of specific sequences.

This study identified the specific regulatory mechanism of *fmtA* transcription by VraR under oxacillin treatment. The VraR binding site A2 in the *fmtA* promoter is highly conserved with the R1 VraR binding site in the *vraSR* promoter, suggesting that this conservation could be a general feature in the VraSR regulon family. The lower amount of conservation in the *sgtB* and *pbp2* promoters, however, also indicates that VraR may have other types of binding sites or different regulatory mechanisms for different VraSR regulon genes. The important role that the VraSR two-component system plays in resistance to environmental stress highlights the need to understand all VraR-mediated regulatory mechanisms.

VraR, together with other factors, may coordinate the regulation of *fmtA* under the influence of cell-wall stressors (Sengupta et al. 2012; Zhao et al. 2012), so the identification of these other factors and their interactions would be a goal worth further research. The *murZ* promoter may be similar to the *fmtA* and *vraSR* promoters, and experiments similar to those in the present study could be designed to confirm this hypothesis. The specific VraR binding sites in the *sgtB* promoter should be determined, perhaps by EMSAs and DNase I footprinting assays where the VraR-protected regions are fragmented into shorter sequences. *pbp2*, though, has multiple transcription start sites and

shares the same operon with its upstream gene *recU* (Pinho et al. 1998), which would complicate the determination of the transcription start sites of *pbp2*. New primers would be required for primer-extension assays in the absence/presence of oxacillin treatment. The lack of conserved VraR binding sites in the *pbp2* promoter is another challenge, so EMSAs and DNase I footprinting assays with shorter fragments could help to identify new VraR binding motifs.

References

Barber M, Rozwadowska-Dowzenko M. 1948. Infection by penicillinresistant staphylococci. 2:641–644.

Belcheva A, Golemi-Kotra D. 2008. A close-up view of the VraSR two-component system. A mediator of *Staphylococcus aureus* response to cell wall damage. J Biol Chem. 283(18):12354-12364.

Belcheva A, Verma V, Golemi-Kotra D. 2009. DNA-binding activity of the vancomycin resistance associated regulator protein VraR and the role of phosphorylation in transcriptional regulation of the vraSR operon. Biochemistry. 48(24):5592-5601.

Bernal P, Lemaire S, Pinho MG, Mobashery S, Hinds J, Taylor PW. 2010. Insertion of epicatechin gallate into the cytoplasmic membrane of methicillin-resistant *Staphylococcus aureus* disrupts penicillin-binding protein (PBP) 2a-mediated β-lactam resistance by delocalizing PBP2. J Biol Chem. 285(31):24055-24065.

Blake KL, O'Neill AJ, Mengin-Lecreulx D, Henderson PJ, Bostock JM, Dunsmore CJ, Simmons KJ, Fishwick CW, Leeds JA, Chopra I. 2009. The nature of *Staphylococcus aureus* MurA and MurZ and approaches for detection of peptidoglycan biosynthesis inhibitors. Mol Microbiol. 72(2):335-343.

Boles BR, Thoendel M, Roth AJ, Horswill AR. 2010. Identification of genes involved in polysaccharide-independent *Staphylococcus aureus* biofilm formation. PLoS One. 5(4):e10146.

Bondi A Jr, Dietz CC. 1945. Penicillin resistant staphylococci. Proc Soc Exp Biol Med. 60:55–58.

Boyle-Vavra S, Yin S, Challapalli M, Daum RS. 2003. Transcriptional induction of the penicillin-binding protein 2 gene in *Staphylococcus aureus* by cell wall-active antibiotics oxacillin and vancomycin. Antimicrob Agents Chemother. 47(3):1028-1036.

Centers for Disease Control and Prevention (CDC). 2002. *Staphylococcus aureus* resistant to vancomycin--United States, 2002. MMWR Morb Mortal Wkly Rep. 51(26):565-567.

Centers for Disease Control and Prevention (CDC). 2002. Vancomycin-resistant *Staphylococcus aureus*--Pennsylvania, 2002. MMWR Morb Mortal Wkly Rep. 51(40):902.

de Lencastre H, de Jonge BL, Matthews PR, Tomasz A. 1994. Molecular aspects of methicillin resistance in *Staphylococcus aureus*. J Antimicrob Chemother. 33(1):7-24.

Deurenberg RH, Stobberingh EE. 2008. The evolution of *Staphylococcus aureus*. Infect Genet Evol. 8(6):747-763.

Diekema DJ, Pfaller MA, Schmitz FJ, Smayevsky J, Bell J, Jones RN, Beach M; SENTRY Partcipants Group. 2001. Survey of infections due to Staphylococcus species: frequency of occurrence and antimicrobial susceptibility of isolates collected in the United States, Canada, Latin America, Europe, and the Western Pacific region for the SENTRY Antimicrobial Surveillance Program, 1997-1999. Clin Infect Dis. 32 Suppl 2:S114-S132.

Dinges MM, Orwin PM, Schlievert PM. 2000. Exotoxins of *Staphylococcus aureus*. Clin Microbiol Rev. 13(1):16-34.

Du W, Brown JR, Sylvester DR, Huang J, Chalker AF, So CY, Holmes DJ, Payne DJ, Wallis NG. 2000. Two active forms of UDP-N-acetylglucosamine enolpyruvyl transferase in gram-positive bacteria. J Bacteriol. 182(15):4146-4152.

Fan X, Liu Y, Smith D, Konermann L, Siu KW, Golemi-Kotra D. 2007. Diversity of penicillin-binding proteins. Resistance factor FmtA of *Staphylococcus aureus*. J Biol Chem. 282(48):35143-35152.

Finland M. 1955. Emergence of antibiotic-resistant bacteria. N Engl J Med. 253: 909–922; contd.

Francis KP, Joh D, Bellinger-Kawahara C, Hawkinson MJ, Purchio TF, Contag PR. 2000. Monitoring bioluminescent *Staphylococcus aureus* infections in living mice using a novel *luxABCDE* construct. Infect Immun. 68(6):3594-3600.

Gardete S, Wu SW, Gill S, Tomasz A. 2006. Role of VraSR in antibiotic resistance and antibiotic-induced stress response in *Staphylococcus aureus*. Antimicrob Agents Chemother. 50(10):3424-3434.

Harraghy N, Kormanec J, Wolz C, Homerova D, Goerke C, Ohlsen K, Qazi S, Hill P, Herrmann M. 2005. *sae* is essential for expression of the *staphylococcal adhesins* Eap and Emp. Microbiology. 151(Pt 6):1789-1800.

Hiramatsu K, Aritaka N, Hanaki H, Kawasaki S, Hosoda Y, Hori S, Fukuchi Y, Kobayashi I. 1997. Dissemination in Japanese hospitals of strains of *Staphylococcus aureus* heterogeneously resistant to vancomycin. Lancet. 350(9092):1670-1673.

Jevons MP. 1961. “Celbenin”-resistant staphylococci. Br Med J. 1:124–125.

Kawada-Matsuo M, Yoshida Y, Nakamura N, Komatsuzawa H. 2011. Role of two-component systems in the resistance of *Staphylococcus aureus* to antibacterial agents. Virulence. 2(5):427-430.

Kluytmans J, van Belkum A, Verbrugh H. 1997. Nasal carriage of *Staphylococcus aureus*: epidemiology, underlying mechanisms, and associated risks. Clin Microbiol Rev. 10(3):505-520.

Komatsuzawa H, Ohta K, Labischinski H, Sugai M, Suginaka H. 1999. Characterization of *fmtA*, a gene that modulates the expression of methicillin resistance in *Staphylococcus aureus*. Antimicrob Agents Chemother. 43(9):2121-2125.

Komatsuzawa H, Sugai M, Ohta K, Fujiwara T, Nakashima S, Suzuki J, Lee CY, Suginaka H. 1997. Cloning and characterization of the *fmt* gene which affects the methicillin resistance level and autolysis in the presence of triton X-100 in methicillin-resistant *Staphylococcus aureus*. Antimicrob Agents Chemother. 41(11):2355-2361.

Kuroda M, Kuroda H, Oshima T, Takeuchi F, Mori H, Hiramatsu K. 2003. Two-component system VraSR positively modulates the regulation of cell-wall biosynthesis pathway in *Staphylococcus aureus*. Mol Microbiol. 49(3):807-821.

Kuroda M, Ohta T, Uchiyama I, Baba T, Yuzawa H, Kobayashi I, Cui L, Oguchi A, Aoki K, Nagai Y et al. 2001. Whole genome sequencing of meticillin-resistant *Staphylococcus aureus*. Lancet. 357(9264):1225-1240.

Laupland KB. 2013. Incidence of bloodstream infection: a review of population-based studies. Clin Microbiol Infect. 19(6):492-500.

Lovering AL, Gretes M, Strynadka NC. 2008. Structural details of the glycosyltransferase step of peptidoglycan assembly. Curr Opin Struct Biol. 18(5):534-543.

Lowy FD. 1998. *Staphylococcus aureus* infections. N Engl J Med. 339(8):520-532.

Lowy FD. 2003. Antimicrobial resistance: the example of *Staphylococcus aureus*. J Clin Invest. 111(9):1265-1273.

M R, D'Souza M, Kotigadde S, Saralaya K V, Kotian M S. 2013. Prevalence of Methicillin Resistant *Staphylococcus aureus* Carriage amongst Health Care Workers of Critical Care Units in Kasturba Medical College Hospital, Mangalore, India. J Clin Diagn Res. 7(12):2697-2700.

McAleese F, Wu SW, Sieradzki K, Dunman P, Murphy E, Projan S, Tomasz A. 2006. Overexpression of genes of the cell wall stimulon in clinical isolates of *Staphylococcus aureus* exhibiting vancomycin-intermediate-*S. aureus*-type resistance to vancomycin. J Bacteriol. 188(3):1120-1133.

Muthaiyan A, Silverman JA, Jayaswal RK, Wilkinson BJ. 2008. Transcriptional profiling reveals that daptomycin induces the *Staphylococcus aureus* cell wall stress stimulon and genes responsive to membrane depolarization. Antimicrob Agents Chemother. 52(3):980-990.

Otto M. 2012. MRSA virulence and spread. Cell Microbiol. 14(10):1513-1521.

Panlilio AL, Culver DH, Gaynes RP, Banerjee S, Henderson TS, Tolson JS, Martone WJ. 1992. Methicillin-resistant *Staphylococcus aureus* in U.S. hospitals, 1975-1991. Infect Control Hosp Epidemiol. 13(10):582-586.

Pérez-Pinera P, Menéndez-González M, Antonio Vega J. 2006. Deletion of DNA sequences of using a polymerase chain reaction based approach. Electron J Biotechnol. 9(5):0-0.

Pinho MG, de Lencastre H, Tomasz A. 1998. Transcriptional analysis of the *Staphylococcus aureus* penicillin binding protein 2 gene. J Bacteriol. 180(23):6077-6081.

Pinho MG, de Lencastre H, Tomasz A. 2001. An acquired and a native penicillin-binding protein cooperate in building the cell wall of drug-resistant staphylococci. Proc Natl Acad Sci U S A. 98(19):10886-10891.

Pinho MG, Filipe SR, de Lencastre H, Tomasz A. 2001. Complementation of the essential peptidoglycan transpeptidase function of penicillin-binding protein 2 (PBP2) by the drug resistance protein PBP2A in *Staphylococcus aureus*. J Bacteriol. 183(22):6525-6531.

Rammelkamp CH, Maxon T. 1942. Resistance of *Staphylococcus aureus* to the action of penicillin. Proc Royal Soc Exper Biol Med. 51:386–389.

Rebets Y, Lupoli T, Qiao Y, Schirner K, Villet R, Hooper D, Kahne D, Walker S. 2014. Moenomycin Resistance Mutations in *Staphylococcus aureus* Reduce Peptidoglycan Chain Length and Cause Aberrant Cell Division. ACS Chem Biol. 9(2):459-467.

Reed P, Veiga H, Jorge AM, Terrak M, Pinho MG. 2011. Monofunctional transglycosylases are not essential for *Staphylococcus aureus* cell wall synthesis. J Bacteriol. 193(10):2549-2556.

Sengupta M, Jain V, Wilkinson BJ, Jayaswal RK. 2012. Chromatin immunoprecipitation identifies genes under direct VraSR regulation in *Staphylococcus aureus*. Can J Microbiol. 58(6):703-708.

Silver LL. 2006. Does the cell wall of bacteria remain a viable source of targets for novel antibiotics? Biochem Pharmacol. 71(7):996-1005.

Skinner D, Keefer CS. 1941. Significance of bacteremia caused by *Staphylococcus aureus*. Arch Intern Med. 68: 851–875.

Stapleton PD, Taylor PW. 2002. Methicillin resistance in *Staphylococcus aureus*: mechanisms and modulation. Sci Prog. 85(Pt 1):57-72.

Stock AM, Robinson VL, Goudreau PN. 2000. Two-component signal transduction. Annu Rev Biochem. 69:183-215.

Stryjewski ME, Corey GR. 2014. Methicillin-resistant *Staphylococcus aureus*: an evolving pathogen. Clin Infect Dis. 58 Suppl 1:S10-S19.

Tu Quoc PH, Genevaux P, Pajunen M, Savilahti H, Georgopoulos C, Schrenzel J, Kelley WL. 2007. Isolation and characterization of biofilm formation-defective mutants of *Staphylococcus aureus*. Infect Immun. 75(3):1079-1088.

Utaida S, Dunman PM, Macapagal D, Murphy E, Projan SJ, Singh VK, Jayaswal RK, Wilkinson BJ. 2003. Genome-wide transcriptional profiling of the response of

Staphylococcus aureus to cell-wall-active antibiotics reveals a cell-wall-stress stimulon. Microbiology. 149(Pt 10):2719-2732.

van Hal SJ, Jensen SO, Vaska VL, Espedido BA, Paterson DL, Gosbell IB. 2012. Predictors of mortality in *Staphylococcus aureus* Bacteremia. Clin Microbiol Rev. 25(2):362-386.

Zhao Y, Verma V, Belcheva A, Singh A, Fridman M, Golemi-Kotra D. 2012. *Staphylococcus aureus* methicillin-resistance factor fmtA is regulated by the global regulator SarA. PLoS One. 7(8):e43998

Appendix

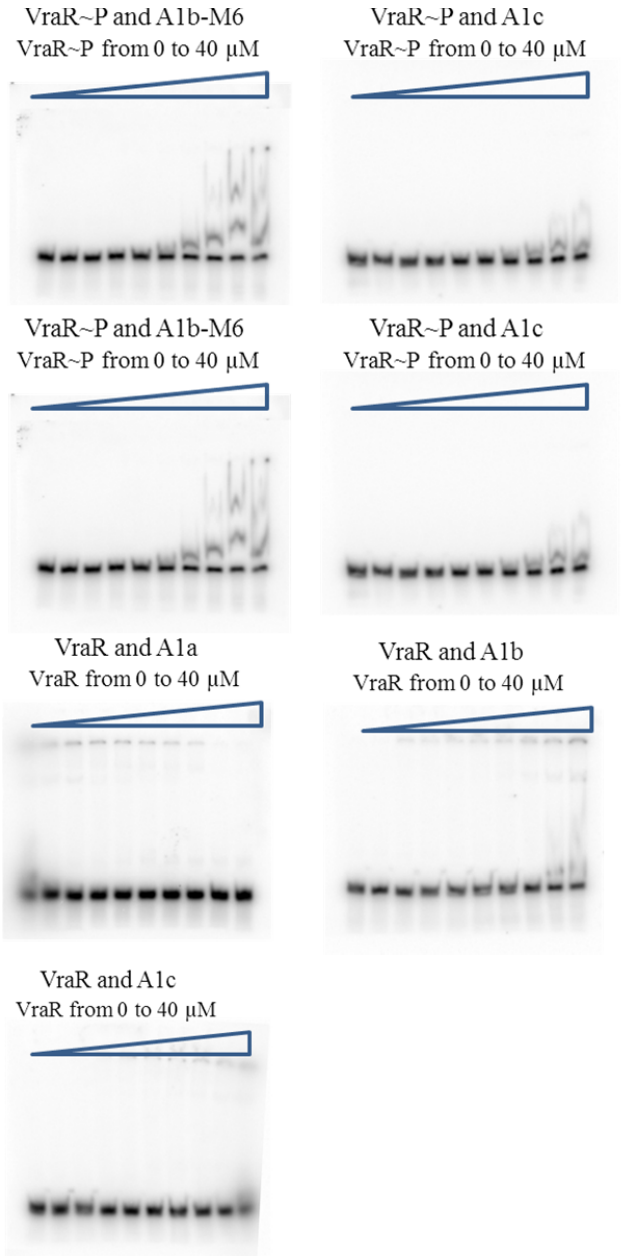

Figure 1 Investigation of VraR/VraR~P binding affinity on A1a A1a-M4, A1b, A1b-M6 and A1c by EMSA. K_d values could not be determined accurately due to the range of available protein concentrations prepared in EMSA procedure.

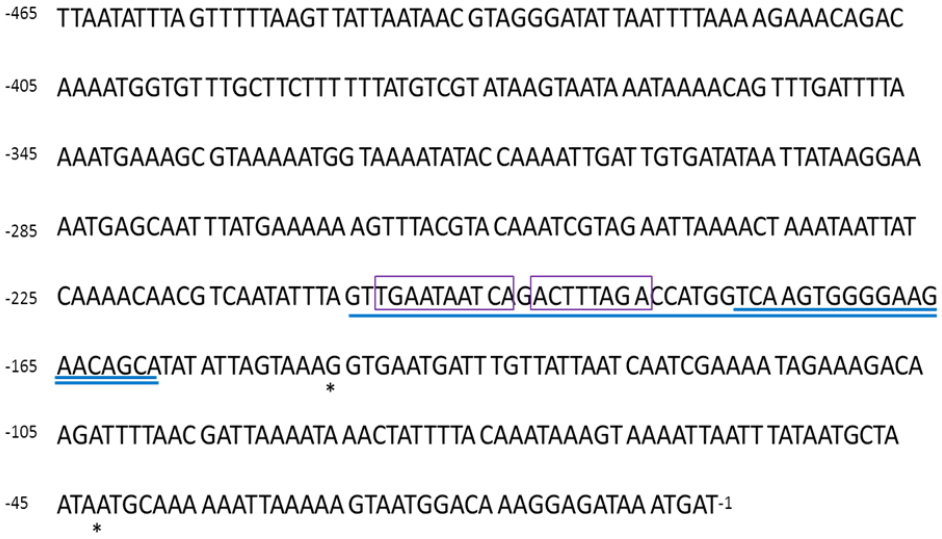

Figure 2a Sequence of P*murZ*. Double-underlined region is protected by VraR~P only in DNase I footprinting assays. Single-underlined region is protected by both VraR and VraR~P. Two conserved VraR binding motifs are highlighted by purple boxes. "*"s indicate predicted transcription start sites of *murZ* according to primer extension assays.

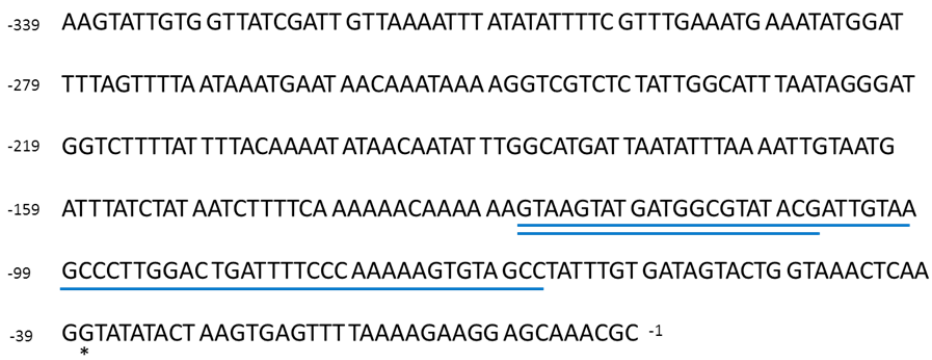

Figure 2b Sequence of P*sgtB*. Double-underlined region is protected by VraR~P only in DNase I footprinting assays. Single-underlined region is protected by both VraR and VraR~P. Two conserved VraR binding motifs are highlighted by purple boxes. "*" indicates the predicted transcription start site of *sgtB* according to primer extension assays.

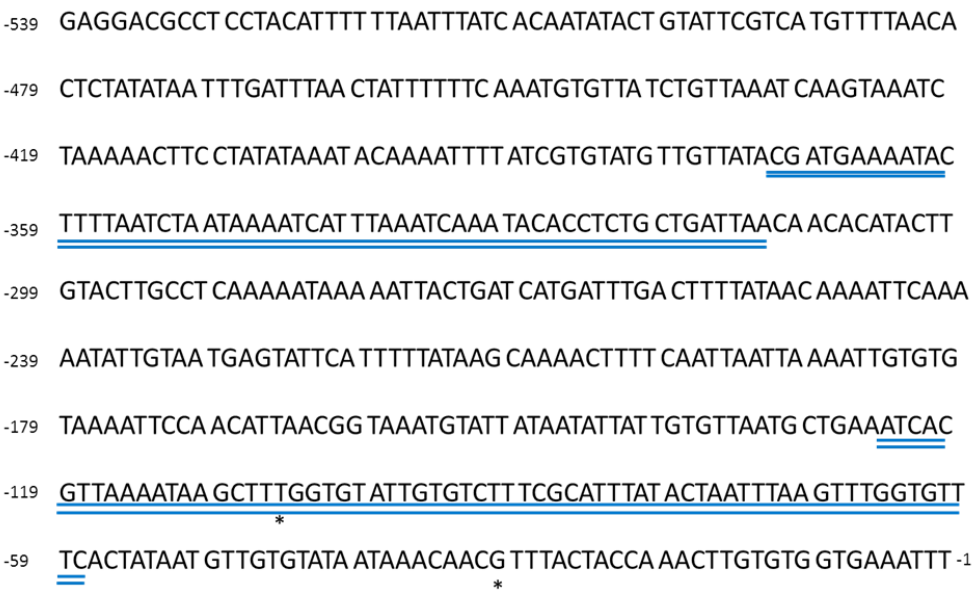

Figure 2c Sequence of P*pbp2*. Double-underlined region is protected by VraR~P only in DNase I footprinting assays. "*"s indicate predicted transcription start sites of *pbp2* according to primer extension assays.

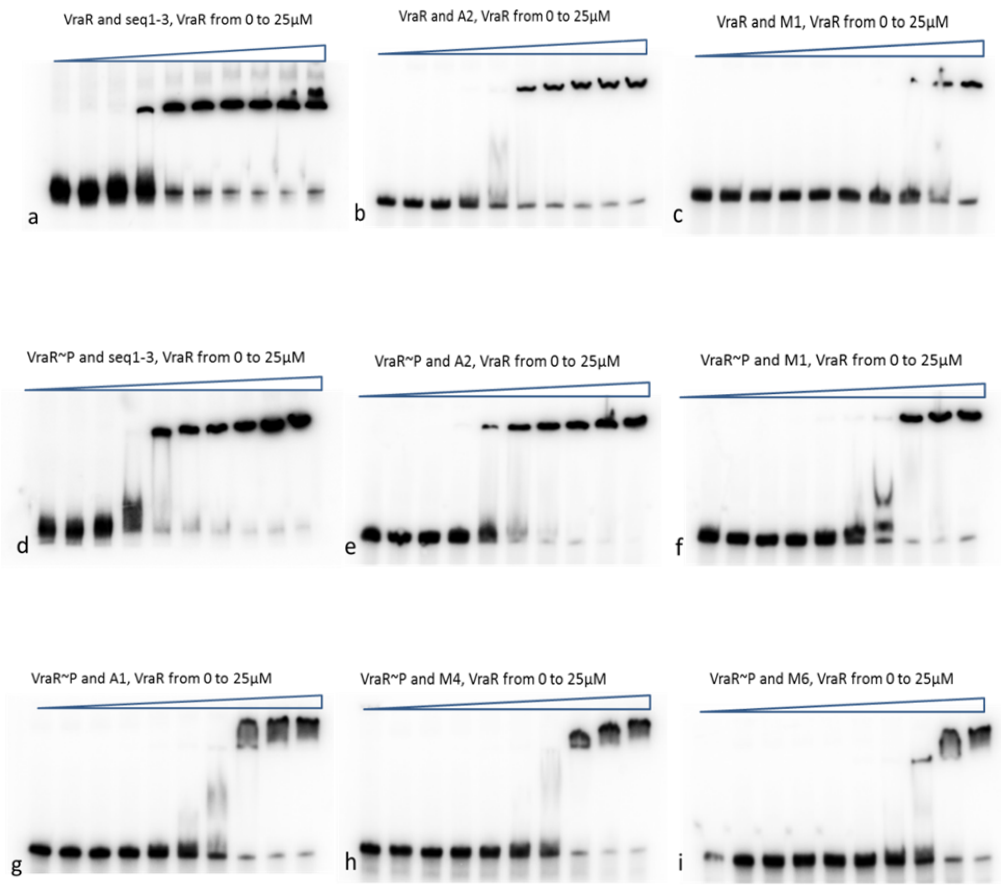

Figure 3. Representive EMSA gels showing the EMSA analysis of the DNA-binding affinities of VraR/VraR~P to seq1-3, A1, A2 and their variants (corresponding to Figure 2.8). a) VraR and seq1-3; b) VraR and A2; c) VraR and A2-M1; d) VraR~P and Seq1-3; e) VraR~P and A2; f) VraR~P and A2-M1; g) VraR~P and A1; h) VraR~P and A1-M4; i) VraR~P and A1-M6.